AN ABSTRACT OF THE THESIS OF

Peter A. Howd for the degree of Master of Science in Oceanography presented on February 10, 1984.

Title: Beach Foreshore Response to Long-Period Waves in the Swash-Zone

Redacted for privacy

Abstract approved: Robert A. Holman

A field experiment designed to test the hypothesis that infragravity and lower frequency waves influence the patterns of erosion and deposition on the beach foreshore has been carried out. The data show coherent fluctuations in the foreshore sediment level which can be related to low frequency wave motions. The fluctuations have heights of up to 6 cm with typical time scales of 8 to 10 minutes. They can be characterized in two ways: by the progression of the fluctuations up the foreshore slope (landward), and by the decrease in the RMS height of the fluctuations as they progress landward. The velocity of migration also changes as the fluctuations progress landward. Analysis of runup time series obtained by time-lapse photography concurrent with the sediment level measurements reveals long-period waves of undetermined origin at frequencies and

phases which strongly suggest that the waves force the original perturbation in sediment level.

In order to better understand the characteristics of these sediment level fluctuations, a numerical model of sediment transport on the foreshore has been developed. Gradients in sediment transport define erosional and depositional areas on the foreshore. Runup velocities were modeled and the results were used in the sediment transport model. The model predicts that any perturbation in foreshore elevation will progress landward while decreasing in amplitude and in velocity, thereby matching the field observations. Relationships between beach slope and the profile response clarified by this model are used to explain the initial formation of the perturbations of sediment level.

Beach Foreshore Response to Long-Period Waves in the Swash-Zone

by

Peter A. Howd

A THESIS

submitted to

Oregon State University

in partial fulfillment of
the requirements for the
degree of

Master of Science

Completed February 10, 1984

Commencement June 1984

APPROVED:

Redacted for privacy

Assistant Professor of Oceanography in charge of major

Redacted for privacy

Dean of College of Oceanography

Redacted for privacy

Dean of Graduate School

Date thesis is presented February 10, 1984

Typed by Peter A. Howd for Peter A. Howd

ACKNOWLEDGMENTS

First and foremost, I would like to thank Dr. Robert Holman for his patience, understanding, and assistance while allowing me to pursue a project of my own design. I would also like to thank Dr. Asbury Sallenger of the U.S. Geological Survey for his encouragement throughout the completion of this study.

There were numerous people who assisted with the collection of the field data. The staff of the Army Corps of Engineers CERC-FRF, directed by Curt Mason, were excellent hosts. The assistance provided by Aage Gribsov, of Oregon State, Bruce Richmond, Tom Reese, and Jeff List of the U.S.G.S., and Bruce Jaffee of the University of Washington is appreciated.

Curt Peterson's input was valuable in many ways. I will fondly recall our discussions out on the porch.

Finally, I would like to thank those people who have made my stay in Corvallis more enjoyable. I trust you all know who you are.

And Kate, thanks for the help and support you have given me throughout all of this. I hope we will have sunnier days in our future.

During my years at Oregon State I was supported by grants from the Office of Naval Research and from the U.S. Geological Survey.

DEDICATION

I would like to dedicate this thesis to my parents for their support during all levels of my education and to the memory of Geoffrey Dimmick, a friend who's enthusiasm for learning and thinking will always serve as an inspiration.

TABLE OF CONTENTS

LIST OF FIGURES

BEACH FORESHORE RESPONSE TO LONG-PERIOD WAVES IN THE SWASH-ZONE

INTRODUCTION

The beach foreshore is a complex environment. There are numerous physical processes which interact to produce the profile observed at any moment in time. The magnitude and nature of the interactions between the foreshore profile and the fluid motions in and on the beach have not been thoroughly examined in light of sediment transport and the resulting patterns of erosion and deposition. While the recent works of Wright et al (1979), Bowen (1980), and Holman and Bowen (1983) demonstrate the role of infragravity (and longer) waves in determining surf-zone profiles, no quantitative study has been made of the role of long waves in determining the foreshore profile. This study reports on one aspect of such an influence.

Previous research on foreshore sedimentation falls into one of several categories. Studies of the formation of rhythmic features of many length scales have been common. Similarly common have been the studies of tidal cycle sedimentation patterns and the role of tides in forcing beach groundwater fluctuations. A third category has been the study of small scale changes in foreshore

elevation and groundwater. This last category of studies has the most bearing on the present investigation.

The study of giant cusps and rhythmic topography is ongoing. Bowen and Inman (1971) briefly mention that giant cusps could be expected in association with crescentic bars. Dolan et al (1979) address the problem in a qualitative manner, showing matches between measured shoreline periodicitites and possible edge wave wavelengths. They present no wave data to substantiate the existence of the suspected edge waves. Komar (1976) discusses the possible modes of rhythmic topography formation and concludes that edge waves provide the best explanation for the original formation, but that later modification, such as that suggested by Sonu (1973), may be important. In all cases, the edge wave hypothesis of formation requires the existence of a drift velocity pattern which is repeated in the longshore direction. Holman and Bowen (1983) discuss the possibilities for generating such patterns.

The formation of beach cusps has received great attention in the literature (Branner, 1900; Evans, 1938; Komar, 1973; Guza and Inman, 1975; Sallenger, 1979). Subharmonic edge waves, the most commonly agreed upon mechanism for the formation of beach cusps, have been observed both in laboratory study (Guza and Inman, 1975) and in the field

(Huntley and Bowen, 1978). However, since incident wave periods only rarely exceed 20 seconds, the subharmonic period is near the lower limit of the interest of this study and thus the influence of subharmonic edge waves generated by the incident gravity waves will be ignored.

Patterns of tidal cycle sedimentation began to be reported in the wake of World War II. Grant (1948) hypothesized that the changes in beach foreshore saturation, due to either tides or storm surges, would cause distinctive changes in the profile. He reasoned that saturated beaches would be more apt to erode since backwash would be undiminished by percolation. On unsaturated beaches, backwash should be diminished by percolation and deposition would be favored. Emery and Foster (1948) studied the change in the foreshore groundwater profile over a tidal cycle and concluded that there was significant exchange of water between the runup and the beach, and that this exchange could influence patterns of erosion and deposition. They calculated the velocity of the effluent groundwater during ebb tide and found it to be sufficient to transport silt.

Duncan (1964) drew upon these conclusions and produced what has become accepted as the best conceptual explanation of foreshore profile change due to tidally induced changes

in the beach groundwater. He found that the beach groundwater level lagged the rise in sea level. The foreshore should then steepen during flood tide as deposition occurs on the unsaturated upper foreshore and erosion occurs on the saturated lower foreshore. During ebb tide the opposite sedimentation pattern holds. The upper foreshore erodes due to the effluence of the groundwater lagging behind the falling tide. His field study supports this hypothesis as do the studies by others (Strahler, 1964; Harrison, 1969).

Studies of small scale morphology on the beach foreshore have been carried out intermittantly. Tanner (1965, 1977) and Broome and Komar (1979) discuss the existence and formation of backwash ripples. These low-aspect ripples (wavelength of about 50 cm, height approximately 1 cm) can be formed under hydraulic jumps in the backwash on gently sloping beaches. They are not characterized by active migration.

Waddell (1973) conducted a study of the interaction between runup processes, beach groundwater and the sediment level response on the foreshore. He measured sediment level at two locations, one meter apart, on the upper foreshore of a low-energy, medium-sand beach. Simultaneously, he measured runup and the beach groundwater at a

series of locations. He found significant fluctuations in sediment level and presented evidence that the oscillations were sandwaves progressing down the foreshore slope due to bedload transport in the backwash phase of the runup. Waddell (1976), referring to the same data, concluded that standing waves in the inner surf-zone were responsible for periodic fluctuations in the beach groundwater level. These groundwater oscillations created "a zone which was periodically saturated or nonsaturated." He then invoked Duncan's (1964) hypothesis and concluded that nonsaturation, or a low in the groundwater oscillation, encouraged deposition and that the subsequent saturation of the location lead to erosion, the result being the observed periodic oscillations. He did not explain how this theory could account for the apparent seaward progression of the oscillations.

Sallenger and Richmond (in press) conducted a field study in Monterey Bay, California with the aim of characterizing sediment level oscillations on a steep, coarse-grained, high-energy foreshore. They measured the sediment level at a series of locations that stretched across the upper two-thirds of the swash-zone, finding sediment level oscillations at periods of six to fifteen minutes occuring at locations above and below the mean swash position. They

reported that the oscillations progressed landward during a period of net seaward transport, thus ruling out the possibility of lower flow regime bedforms such as sand waves. The width of foreshore monitored allowed them to show a landward decrease in the RMS height of the oscillations. They hypothesized that low frequency motions in the groundwater may have had an influence in causing the observed oscillations, but they present no conclusive proof of this.

The purpose of this study was to test two hypotheses regarding foreshore sediment level oscillations with periods on the order of ten minutes. The first of these hypotheses is that infragravity or longer waves are capable of influencing the foreshore profile. The second hypothesis is that the profile response is not limited to the zone of intermittant saturation, groundwater fluctuations playing a lesser role than has been thought.

To test these hypotheses a field experiment was carried out on a high-energy, coarse-grained beach. The location chosen differed from that of Sallenger and Richmond (in press) in that it was on an open coast rather than within a major embayment known to have seiches. The goals of the field study were to document forcing (or non-forcing) of the sediment level oscillations by long period waves, to show that the oscillations are independent of any

long term erosional or depositional trends on the foreshore, and that the oscillations are not directly related to the saturation of the foreshore.

To aid in the interpretation of the field data a numerical model was developed based on the sediment transport equations presented by Bagnold (1963, 1966) and previously adapted to the surf-zone by Bowen (1980), Holman and Bowen (1983), and by Bailard and Inman (1981). The model was helpful in showing how the oscillations migrate and in explaining the observed characteristics of height and velocity decay as the oscillations progressed. The initial formation of the oscillations is explained using a conceptual model which combines elements of the field study and the simulation results.

EXPERIMENT LOCATION AND METHODS

The field experiments were conducted during September 1981 and October 1982 at the U.S. Army Corps of Engineers, Coastal Engineering Research Center (CERC), Field Research Facility (FRF) on the outer banks of North Carolina near the town of Duck (Figure 1). The beach is interrupted only by piers for at least 50 km on either side. The nearest pier (belonging to the FRF complex) is 500 m from the experiment location. The surf-zone morphology in the region of the experiment is characterized by a single linear bar during conditions similar to those of the study periods. The average mid-foreshore slope during the studies was approximately 1:10. The foreshore is composed of medium to coarse sand with an average grain diameter of approximately 1 mm (Figure 2). During the two experiments the waves were oblique to the beach and had significant wave heights very close to 1 m as measured at a waverider buoy anchored in 20 m of water. There was little wind and waves were of the swell type. The tide range was approximately 0.9 m and semidiurnal. Figure 3 summarizes the environmental conditions surrounding the experiments.

On September 19, 1981 19 stakes 1 cm in diameter and

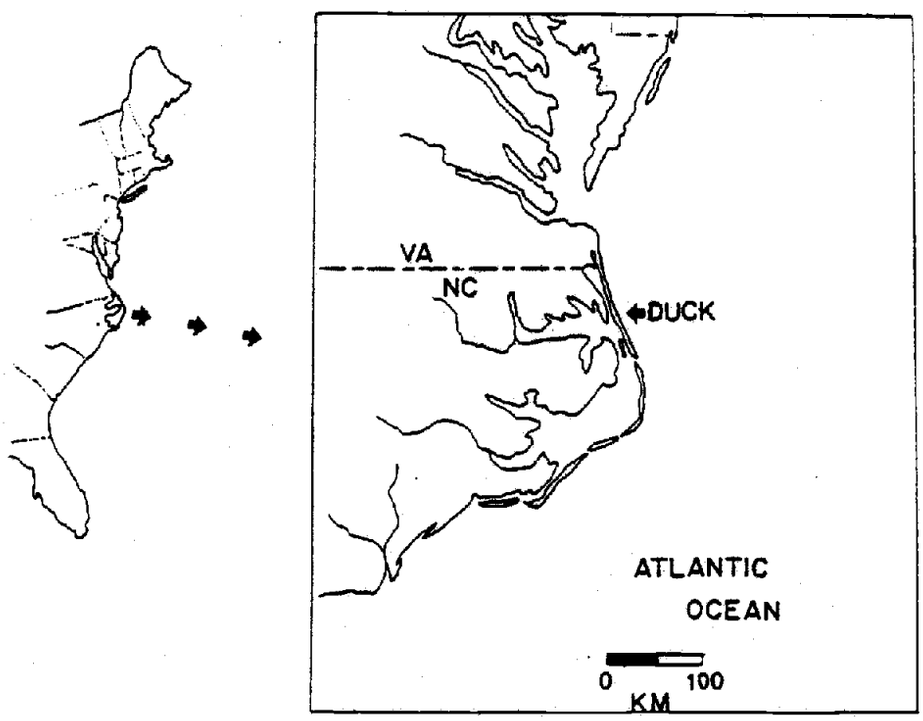

Figure 1. Location map. The field study was conducted at the Coastal Engineering Research Center Field Research Facility just north of the town of Duck, North Carolina. The beach is uninterrupted from Cheseapeake Bay to the north to Oregon Inlet to the south.

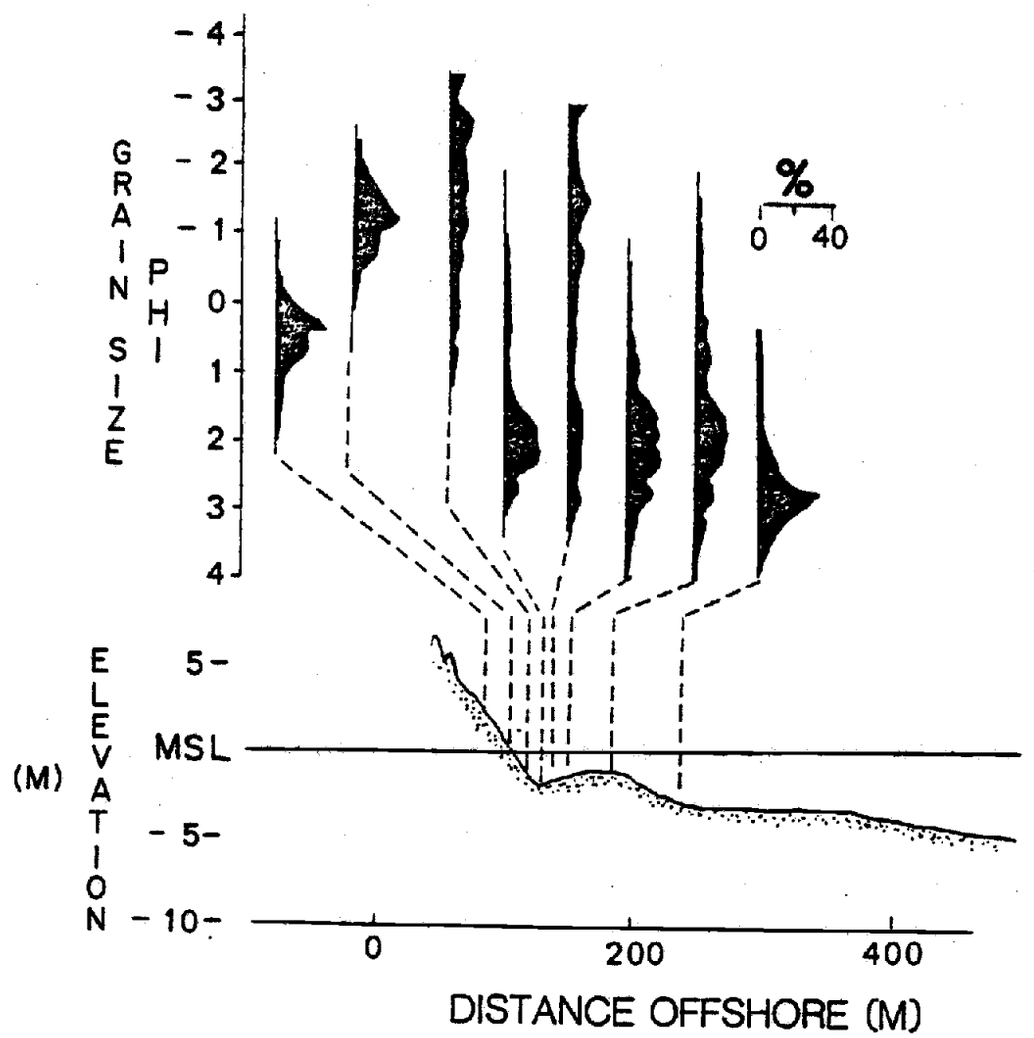

Figure 2. Grain size distribution. Cross-shore grain size distribution on a transect several meters south of the study site on 28 October 1982. The foreshore is composed of sand with an average diameter of approximately 1 mm. Data courtesy of Bill Birkemeier, CERC-FRF.

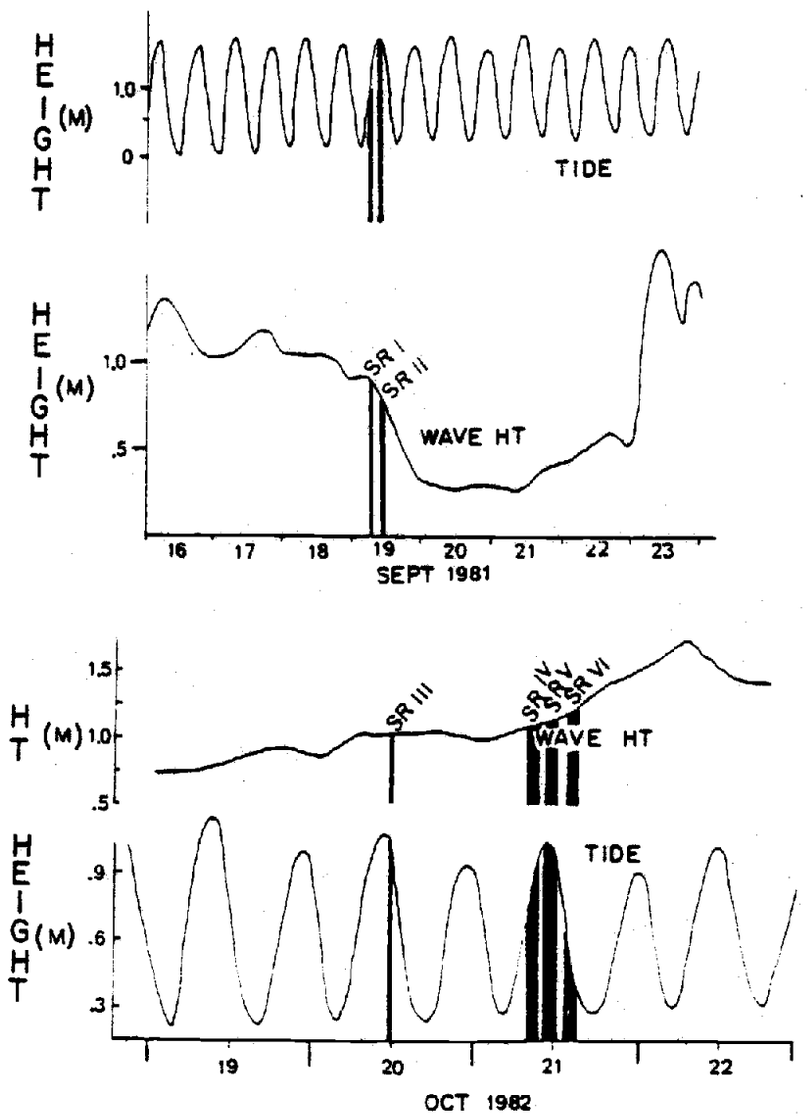

Figure 3. Environmental conditions. The significant wave height was measured by a waverider buoy in 20 m of water. The tides are semidiurnal and have a range of 0.75 to 1.3 meters.

1.5 m long were driven into the foreshore in the locations shown in Figure 4. The foreshore topography was dominated by a series of cusps, one of which is evident from the contours. The primary shore-normal line of eleven stakes had a spacing of 2.0 m. A profile taken that day using the FRF Coastal Research Amphibious Buggy (CRAB) and an infrared rangefinder shows a single bar located in the inner surf-zone (Figure 5).

In October 1982 an array containing eight shore-normal lines of stakes was established on the foreshore (Figure 6). The eight shore-normal lines were spaced 5 m apart. The second line from each end of the grid had shore-normal stake spacings of 2.5 m while the remaining lines had 5 m spacings. The foreshore contours show a remnant cusp in the backshore separated from the active, featureless foreshore by a well defined berm crest. A contour map of the surf-zone topography from 19 October 1982 shows a bar approximately 20 m from shore. The mapping, done by the FRF staff using their CRAB (Birkemeier et al, 1981), shows the bar to be linear along shore. There was little evidence to suggest that there was any appreciable change in the topography over the two day period.

Fluctuations in sediment level relative to the stake tops were measured using a modified meterstick. A hinged

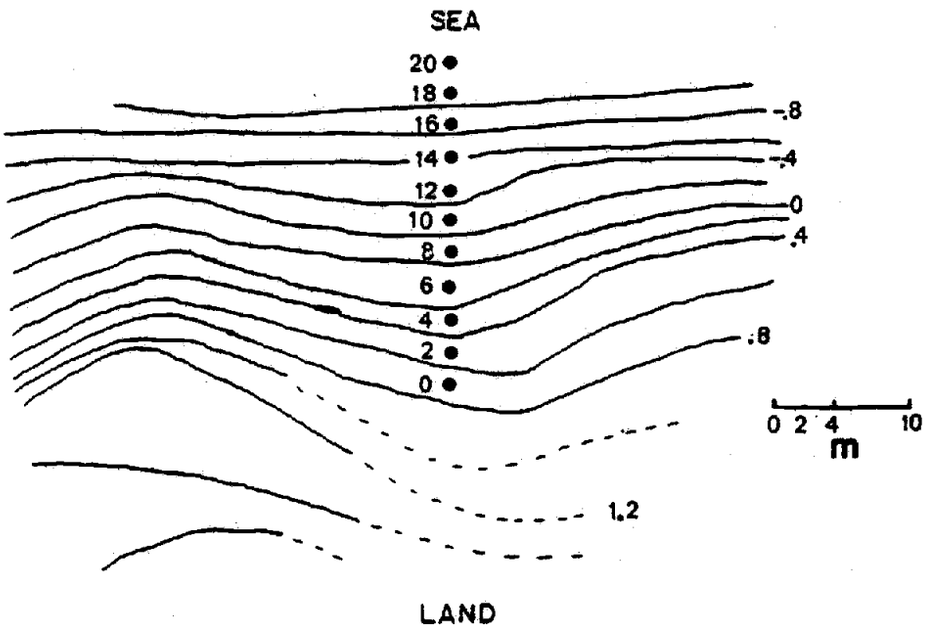

Figure 4. Foreshore topography and stake locations for the 1981 experiment (SR I and SR II). The primary stake transect was located in the trough of a cusp. The stakes are numbered according to their distance seaward from the landwardmost stake and are spaced at 2.0 m intervals.

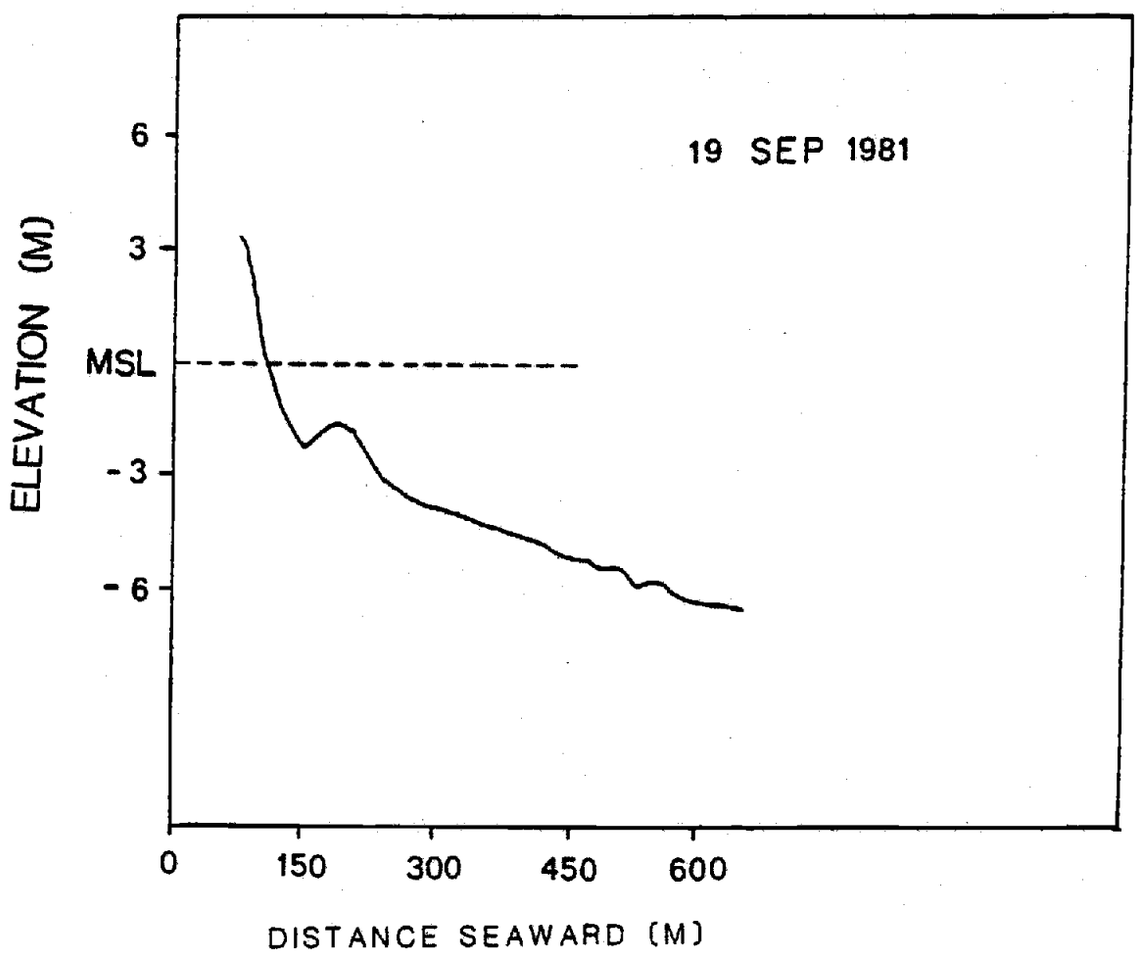

Figure 5. Beach profile, 1981. The profile was taken approximately 10 m south ofthe study site using the FRF CRAB and an infrared rangefinder. The profile shows a single bar located in the inner surf-zone.

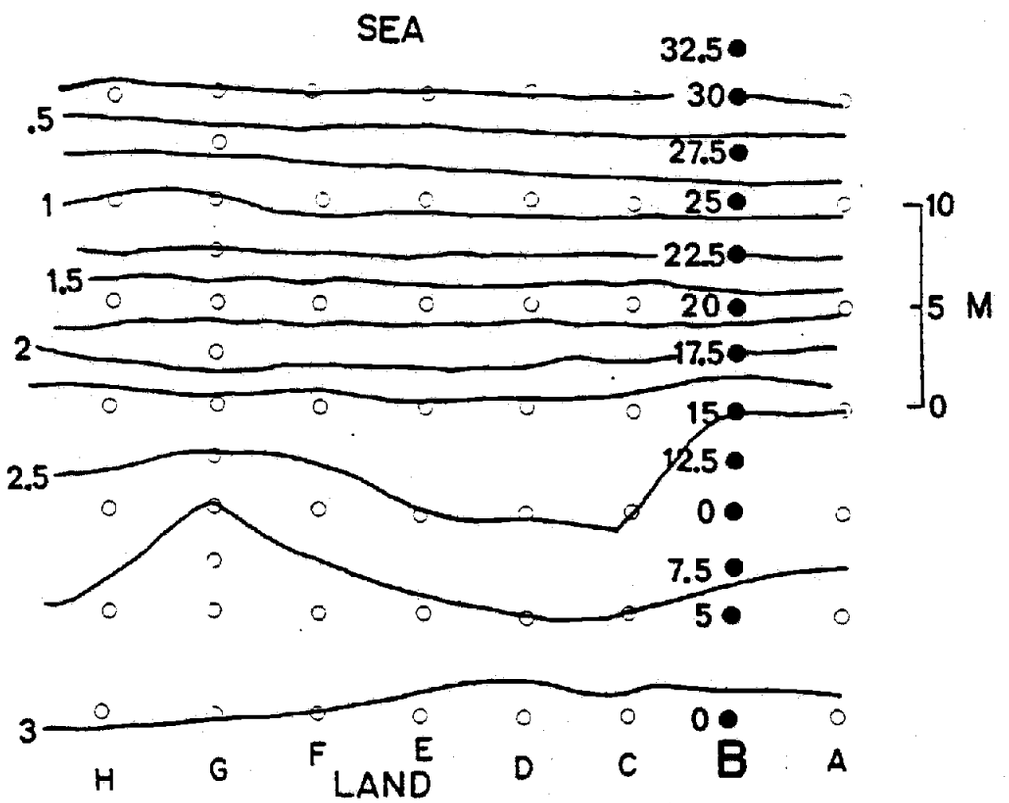

Figure 6. Foreshore topography and stake locations for the 1982 experiment (SR III to SR VI). The B line of stakes were those used in the study. The active portion of the foreshore was seaward of 17.5 m. A remnant cusp was perched landward of the berm crest. The foreshore is linear and has a slope of slightly greater than 1:10.

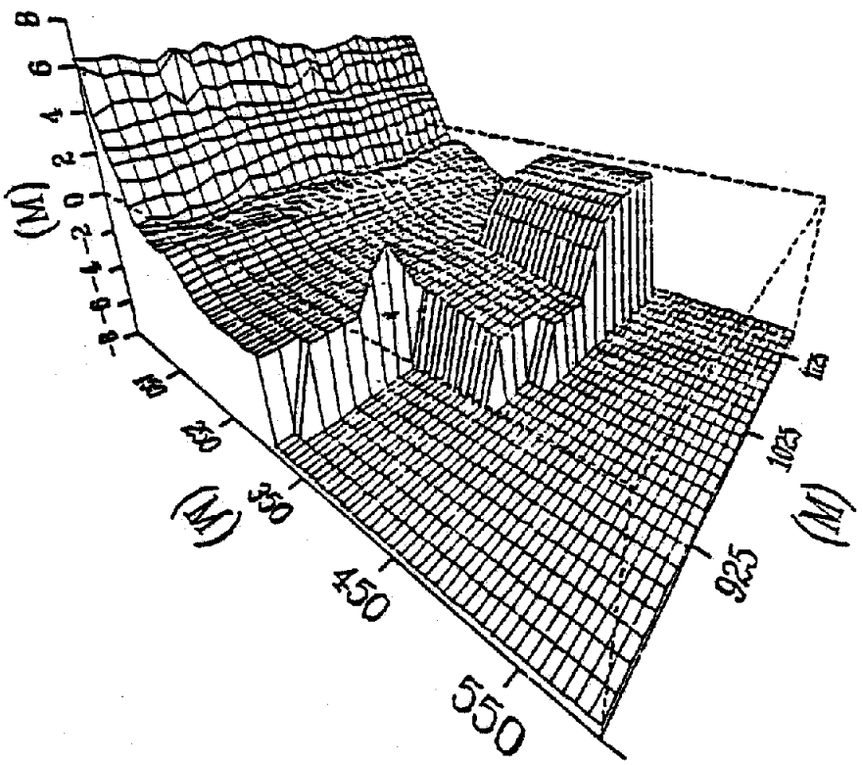

Figure 7. Surf-zone topography on 19 October 1982, one day prior to the data collection. The foreshore stake grid was located in the center of the area shown. The contours show a single quasi-linear bar located in the inner surf-zone. The data and the plot are courtesy of CERC-FRF. The data seaward of 250 m are incomplete which results in the odd contour patterns.

baseplate approximately 10 cm in diameter was affixed to one end of the meterstick to prevent penetration of the sediment surface. A moveable pointer was fitted to the meterstick and was used to determine the length of stake exposed. The stake tops were referenced to a known elevation using an infrared rangefinder. The resolution of the technique, employing different measurers and different metersticks was ± 1.5 mm in the upper swash-zone and ± 2.5 mm in the lower swash-zone. Resolution of the measurements made on stakes not subjected to runup was ± 0.5 mm. The differences are primarily due to the time available to make the measurement and the saturation of the sediment.

During both the 1981 and the 1982 experiments, time-lapse motion pictures were used to record the wave runup on the foreshore. This method allows for digitization of the runup at a series of longshore locations as well as the identification of the saturated portion of the foreshore. The results of a comparison of the film technique and a dual-resistance wire runup meter are presented by Holman and Guza (in press).

The 19 September 1981 experiment consisted of two sixty minute segments, one centered on mid-flood tide, SR I, the second centered on high tide, SR II. The stakes on the primary shore-normal line were measured to the nearest

millimeter at approximately 48 second intervals. Measurements were made after the backwash cycle when the stake was either suberial or the velocity of the water covering the location was low. The landwardmost stakes were measured only after they had been exposed to runup action. The times at which the measurements were made were recorded to the nearest .2 minute (±6 seconds).

The 1982 experiment consisted of one 35 minute segment near high tide on 20 October (SR III) and three 90 minute segments centered on mid-flood, high, and mid-ebb tides on 21 October (SR IV, SR V, and SR VI, respectively). Again, the stakes in a shore-normal line were measured at approximately 48 second intervals after the backwash cycle. Measurements were recorded to the nearest .2 minute. Stakes on the B-line (Figure 6) were those measured most frequently. The number of stakes measured varied according to the number of people measuring and the width of the swash-zone.

FIELD STUDY RESULTS

The results of the data collected during the 19 September 1981 experiment (SR I and SR II) and the data collected on 20 and 21 October 1982 (SR III through SR VI) are presented in Figures 8 through 13 as plots of the change in sediment level at a location versus time for the primary, shore-normal lines of stakes. The stakes are numbered using their distance from the landward baseline, thus the higher numbers refer to stakes further seaward. Several characteristics are immediately visible. All data show sediment level fluctuations superimposed on longer term trends. The trends are due either to the tidal cycle sedimentation patterns or to longer scale foreshore evolution such as changes related to storm cycles. On a shorter time scale, the fluctuations appear to be somewhat periodic, decreasing in amplitude in a landward direction from a maximum height of greater than 6 cm to near zero. The stake locations on the lower foreshore show fluctuations occuring more rapidly than those at the upper, landward stakes. The fluctuations also appear to be progressive, particularly those in Figures 8 and 10, and are coherent over at least 15 m in a longshore direction.

Statistical analysis quantifies these visual observations. The records were processed using linear interpola-

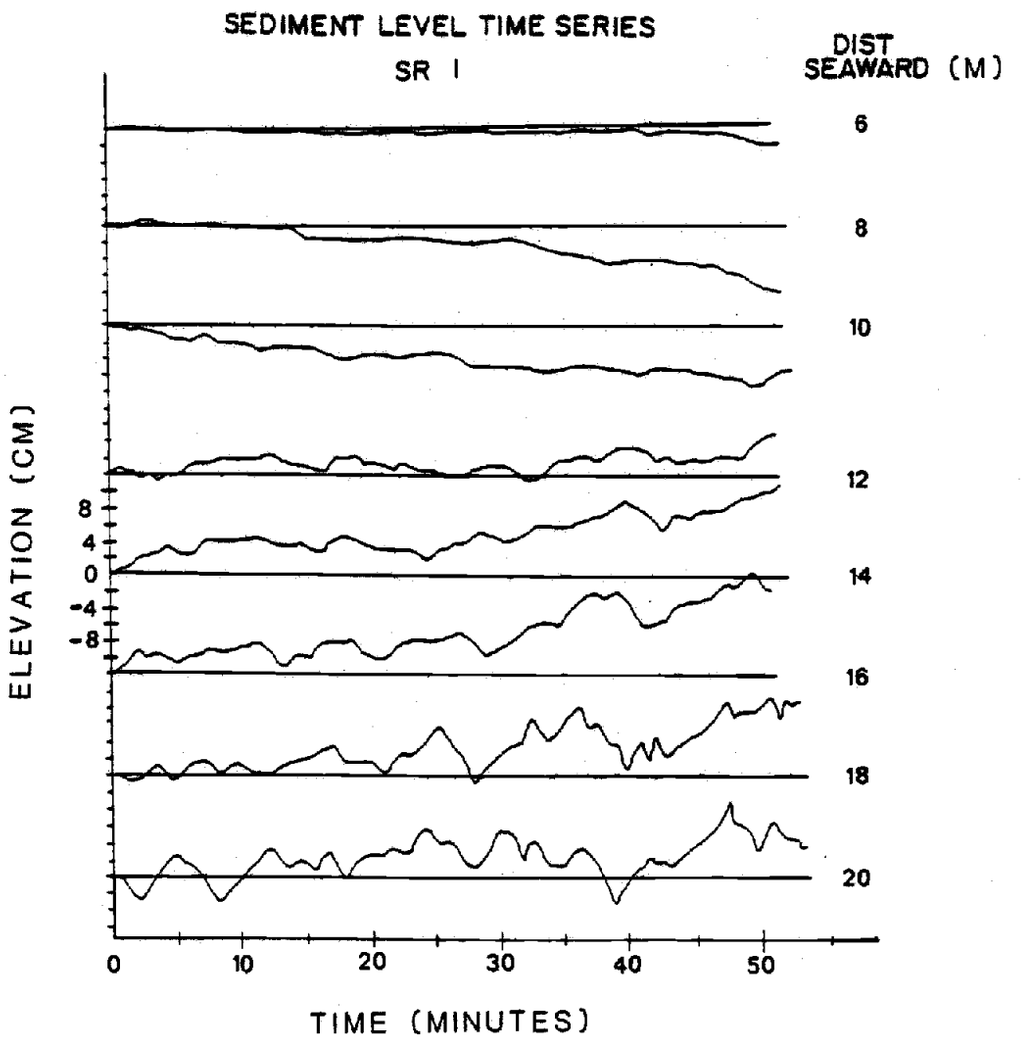

Figure 8. Sediment level time series, SR I. The time series are reported relative to the initial elevation at each location. Several trends are obvious. There are trends in the records, the oscillations decrease in amplitude in a landward direction, and they seem to progress.

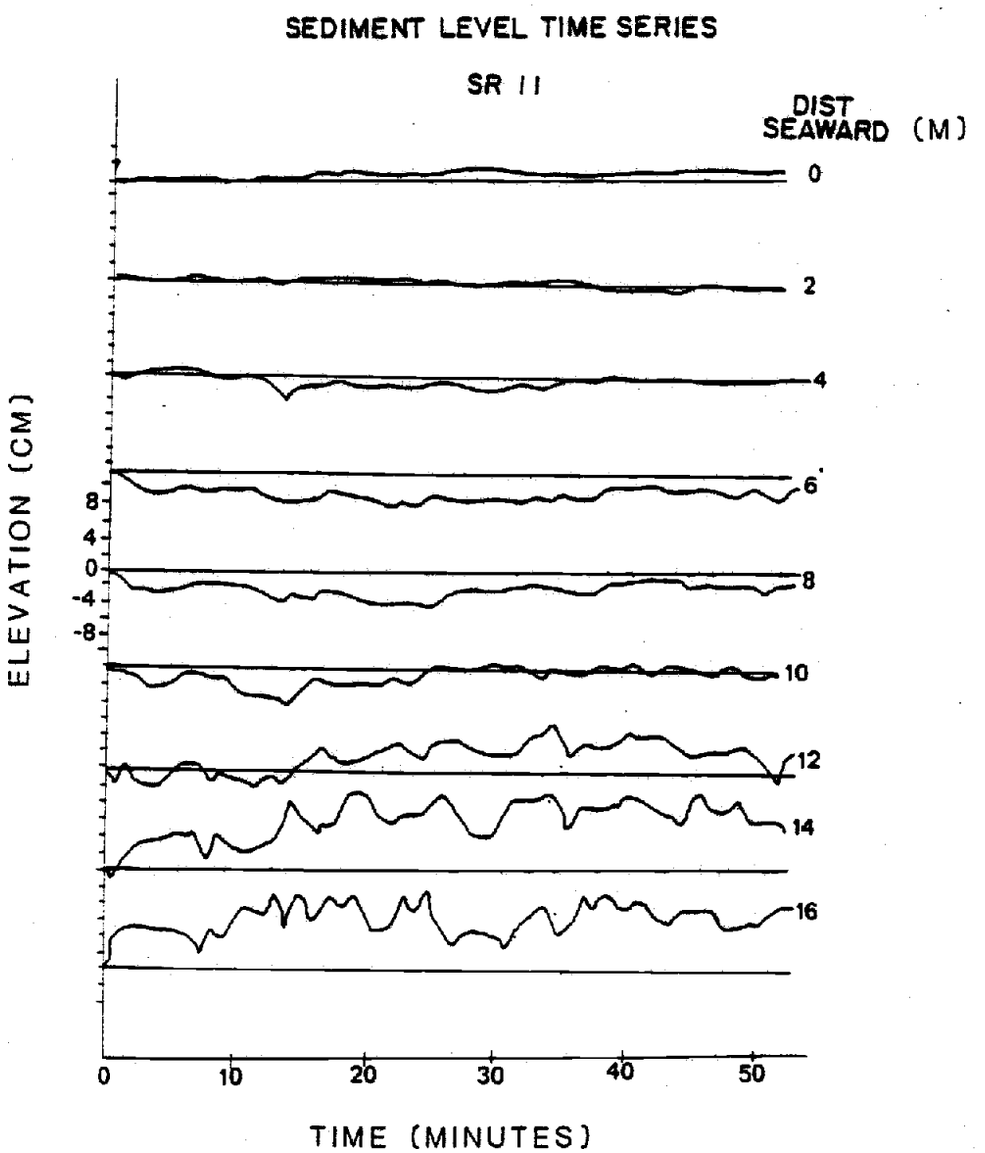

Figure 9. Sediment level time series, SR II. Note the trends and that the fluctuations decrease in height landward.

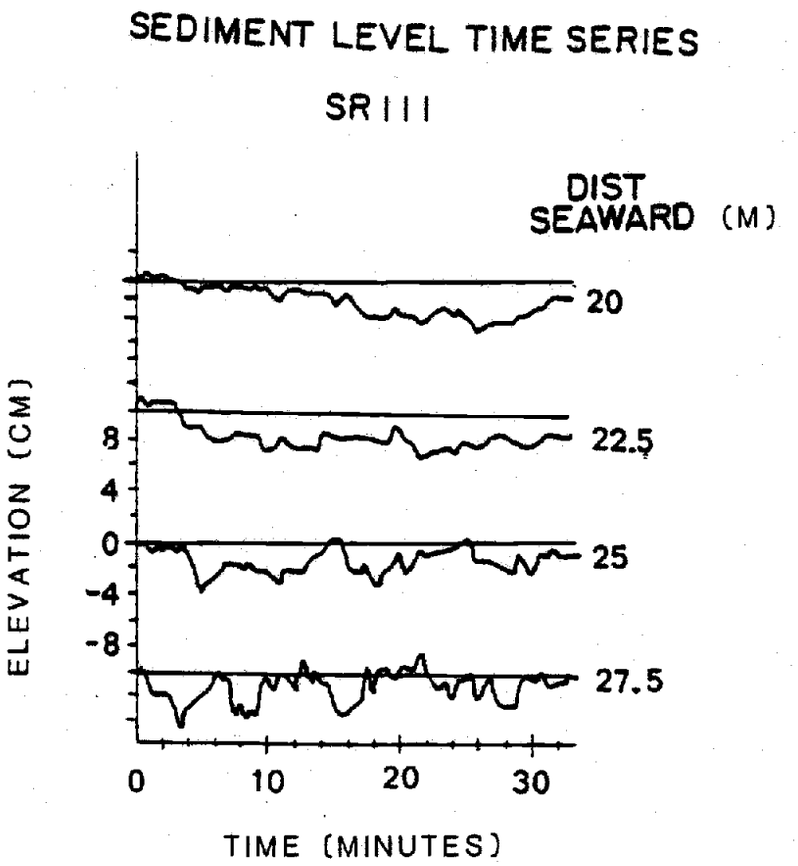

Figure 10. Sediment level time series, SR III.

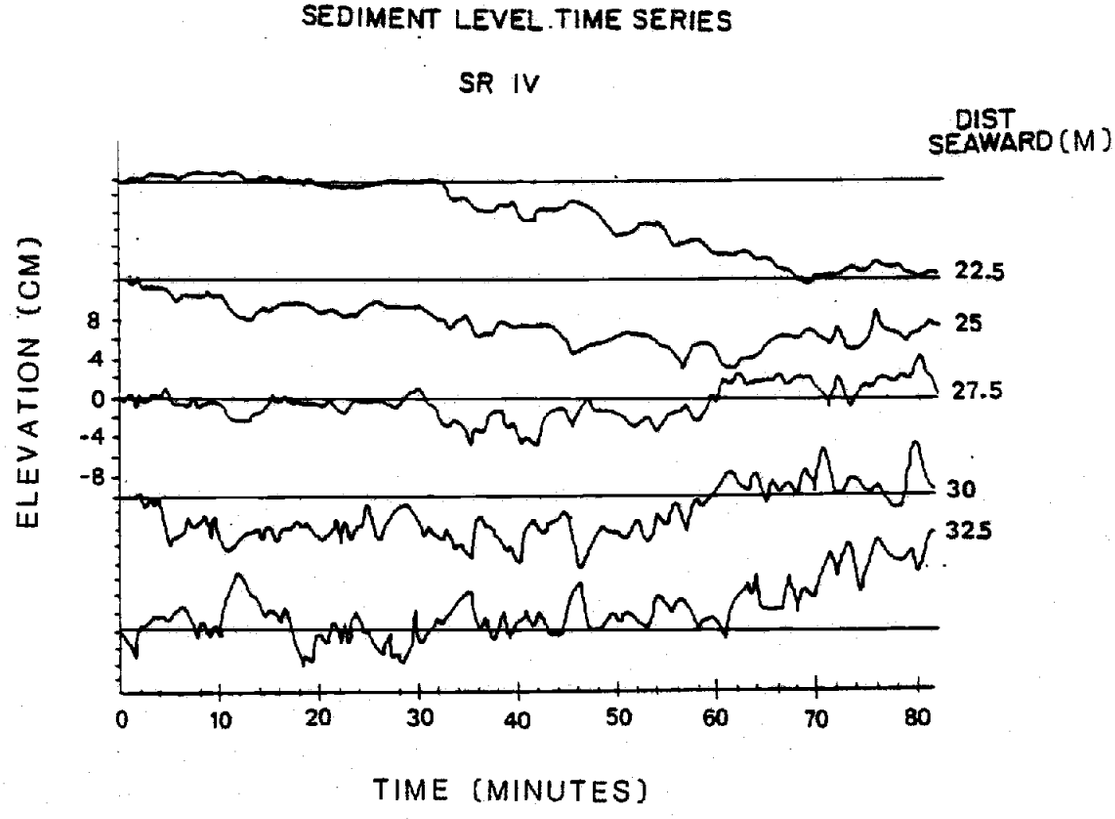

Figure 11. Sediment level time series, SR IV.

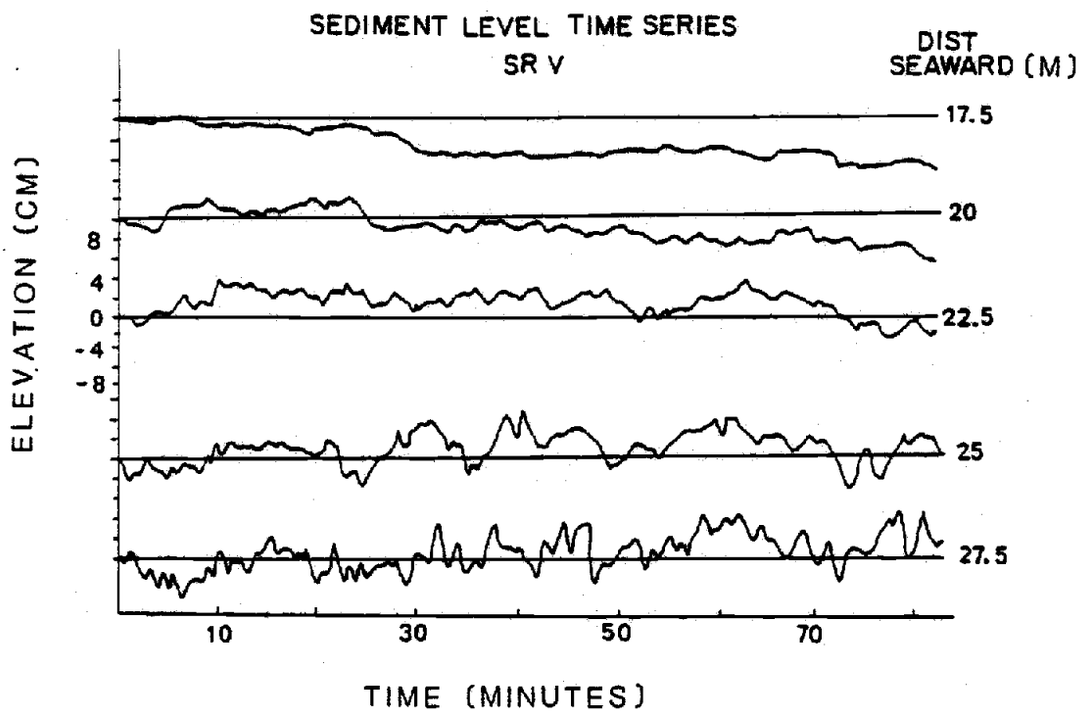

Figure 12. Sediment level time series, SR V.

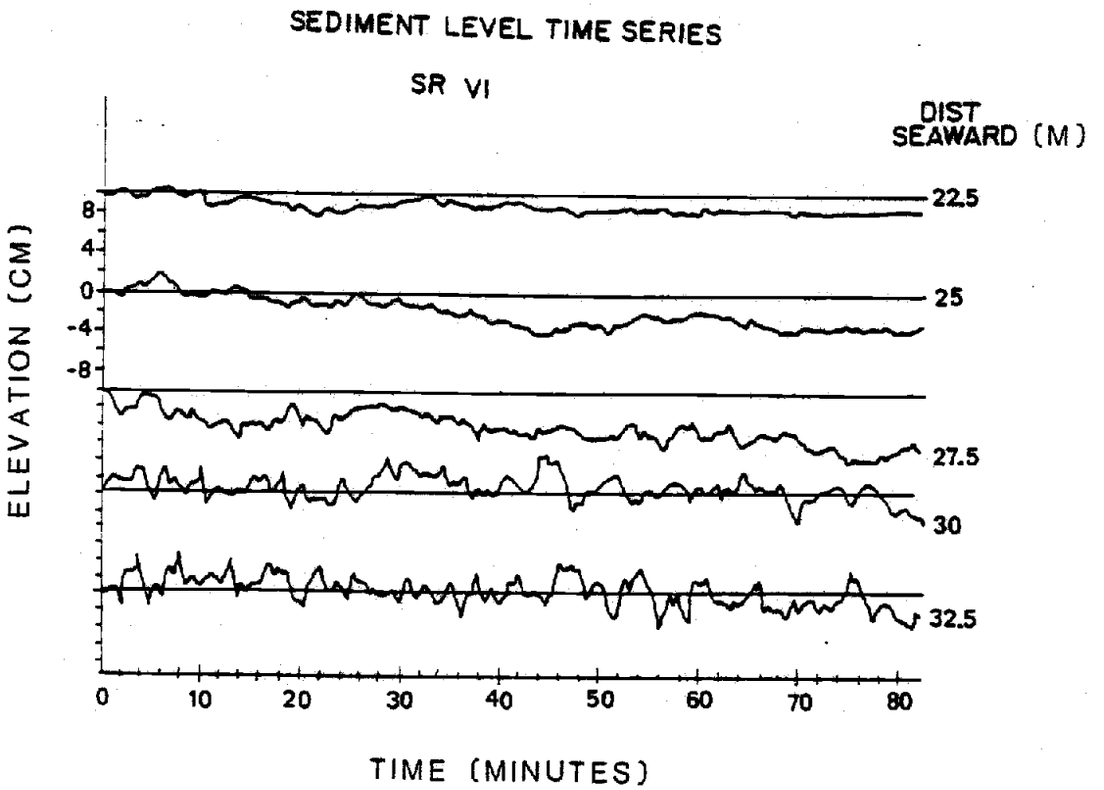

Figure 13. Sediment level time series, SR VI.

tion to give time series with a constant interval of 12 seconds. The trend and mean were then removed so that they would not mask the analysis of the oscillations.

Figure 14 presents the relationship between root-mean-square (RMS) height and the distance from the top of the swash action for the 1982 data. The RMS heights of the fluctuations were computed as two times the standard deviation of the record. All segments show the landward decrease in the RMS height of the oscillations, which ranged from a maximum of > 4 cm at the seawardmost stake to near 0 cm for the landward stakes.

Crosscorrelation analysis was used to compare the detrended and demeaned time series. This analysis computes the correlation between two series of data at a series of lag times (Davis, 1973). It is not a frequency specific calculation as is the measure of coherence reported in association with cross spectral analysis. The lag associated with the maximum value in crosscorrelation is a measure of the shift of one series which results in the two series being most alike.

Figures 15 through 20 summarize the results of the analysis as contour plots of crosscorrelation as a function of distance and lag time. Negative lags indicate that events at that location preceeded the events at the refer-

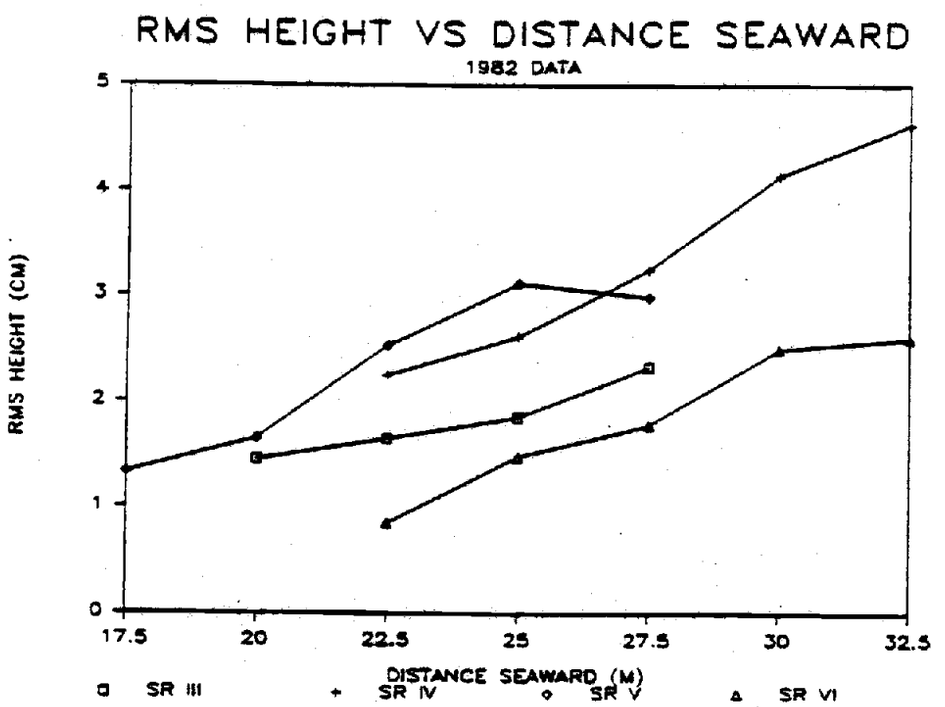

Figure 14. RMS heights of the sediment level fluctuations versus distance seaward for the 1982 data. Note the decrease in the RMS height in a landward direction for all the runs. The RMS height was computed as twice the standard deviation of the run.

ence stake. The contours indicate a change from negative lags for stakes below the reference point to positive lags above. This indicates landward progression of the fluctuations. Table I shows the results for each stake versus its immediate neighbor, either 2.0 or 2.5 m away. In all cases the lag is that of the seaward stake with respect to the landward stake. A negative lag indicates that events at the landward stake follow their occurence at the seaward stake, or that there has been a landward progression.

The flood-tide data, SR I and SR IV, both show lags which indicate landward migration of the oscillations (Figures 15 and 18). Adjacent stakes in the mid-foreshore have crosscorrelation maxima ranging from .54 to .79 (Table I), while stakes which are farther from one another have values which range from essentially zero to .43. The lowered crosscorrelation values between non-adjacent stakes are primarily due to the loss of the high frequency oscillations present in the records obtained in the lower swash-zone.

The three high-tide segments also have maxima associated with landward migration of the fluctuations (Figures 16, 17, and 19). Again, the values of the maxima are highest between adjacent stakes and decrease for non-adjacent stakes due to the loss of higher frequency fluc-

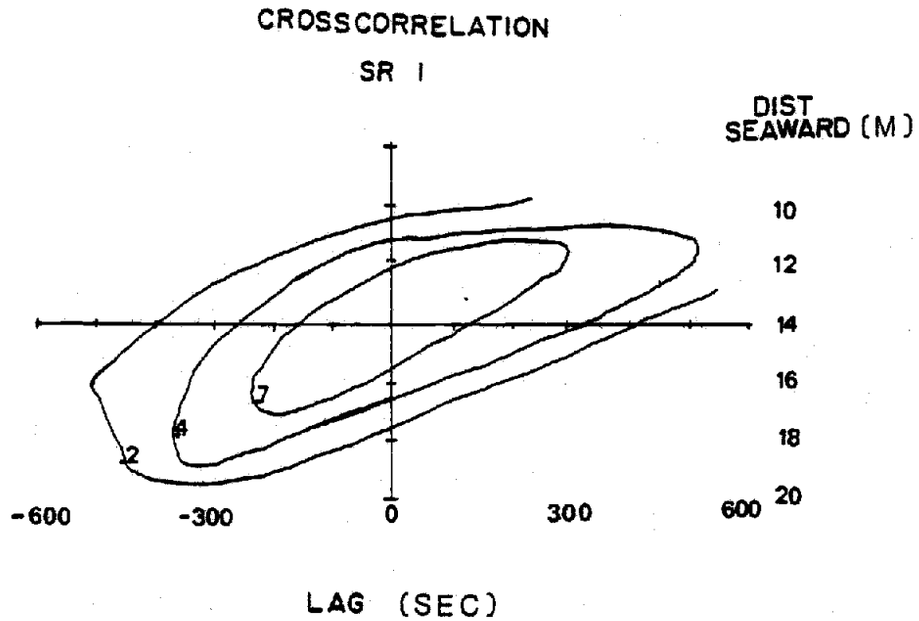

Figure 15. Crosscorrelation vs. time and distance for SR I. The crosscorrelation was computed between each time series and the time series from the stake located 14 m seaward of the baseline. The elongation of the contours from the lower left to upper right indicates a landward progression of the fluctuations. Values > 0.2 are significant at > 95% level for all lags shown in this and the following figures.

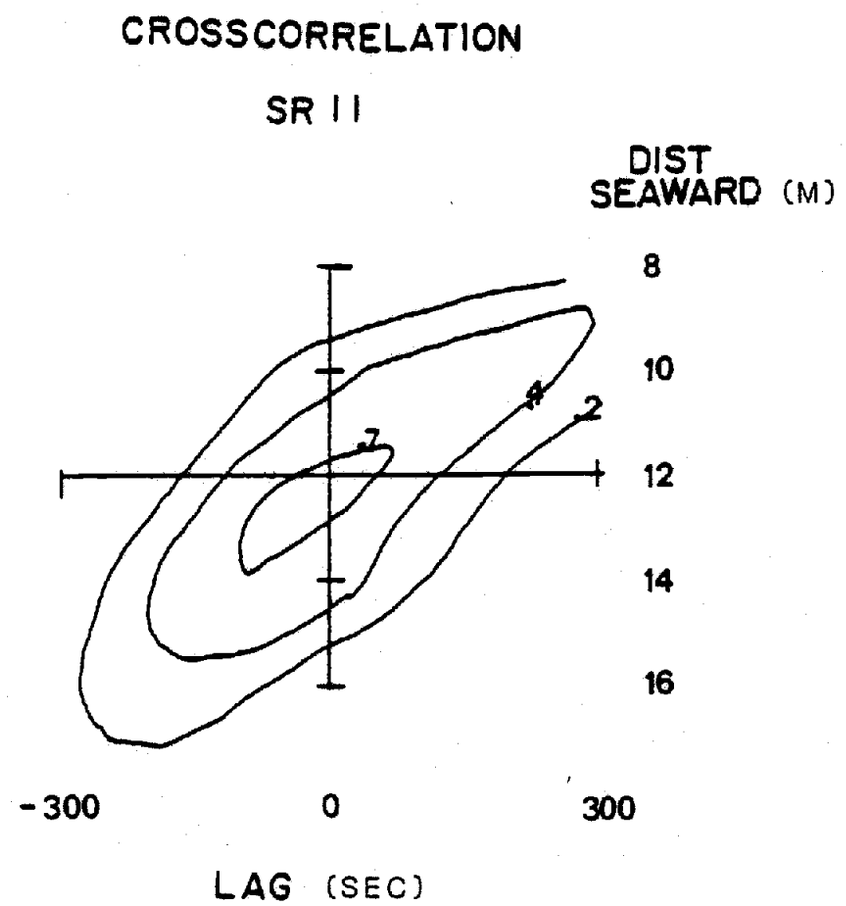

Figure 16. Crosscorrelation vs. time and distance for SR II. The elongation of the contours again indicates landwardprogression. The changes in the slope of the contours suggest changes in the rate of migration.

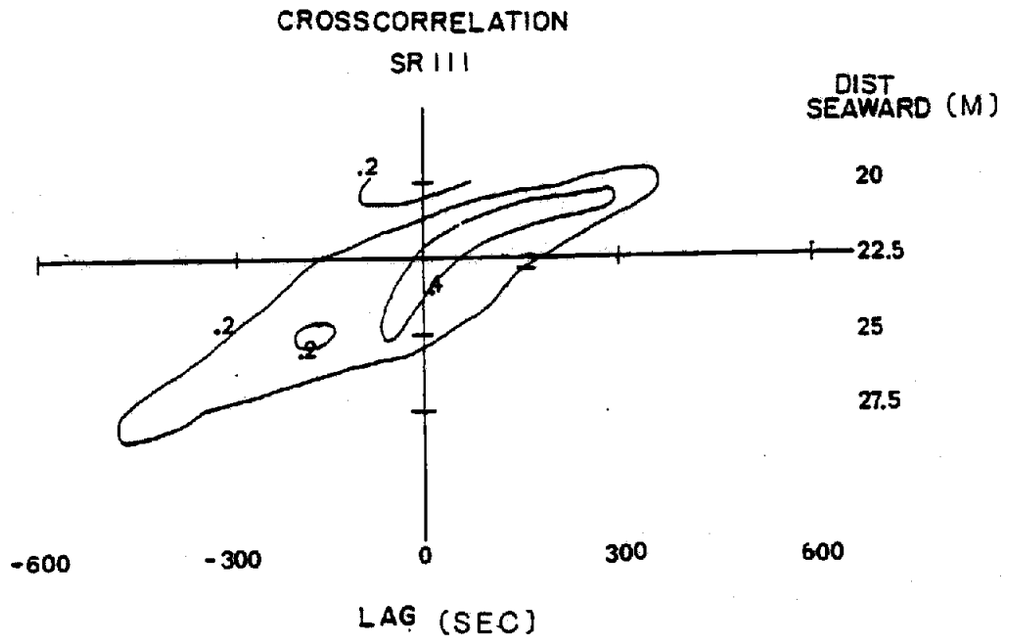

Figure 17. Crosscorrelation vs. time and distance for SR III. Again, landward progression is indicated.

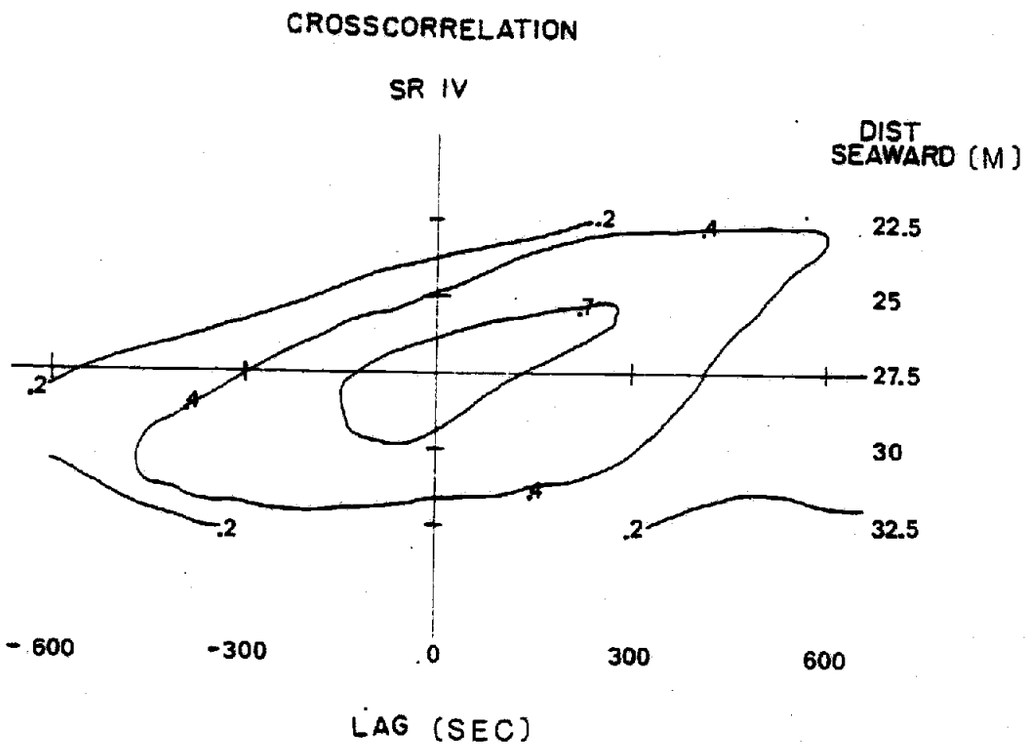

Figure 18. Crosscorrelation vs. time and distance for SR IV.

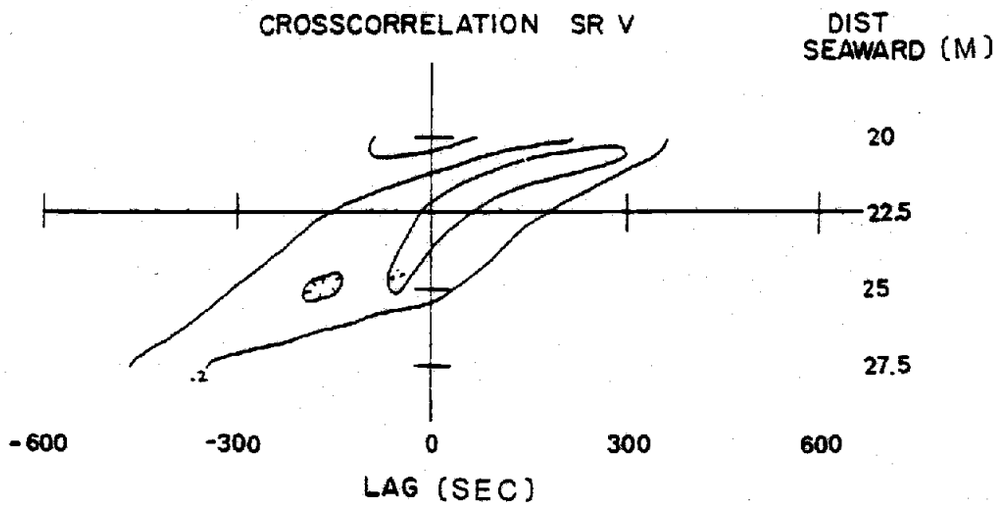

Figure 19. Crosscorrelation vs. time and distance for SR V.

TABLE I: Crosscorrelation results for adjacent stakes. The lags refer to the offset of the seaward stake which results in the highest value for the crosscorrelation coefficient. A positive lag corresponds to landward progression.

		R	Lag
SR I			
	20 m - 18 m	0.40	60 s
	18 m - 16 m	0.63	72 s
	16 m - 14 m	0.79	72 s
	14 m - 12 m	0.78	84 s
	12 m - 10 m	0.50	96 s
SR II			
	16 m - 14 m	0.44	72 s
	14 m - 12 m	0.67	108 s
	12 m - 10 m	0.43	156 s
	10 m - 8 m	0.56	60 s
	8 m - 6 m	0.78	24 s
SR III			
	27.5 m - 25.0 m	0.58	108 s
	25.0 m - 22.5 m	0.40	60 s
	22.5 m - 20.0 m	0.32	300 s
SR IV			
	32.5 m - 30.0 m	0.22	192 s
	30.0 m - 27.5 m	0.70	84 s
	27.5 m - 25.0 m	0.55	228 s
	25.0 m - 22.5 m	0.30	456 s
SR V			
	27.5 m - 25.0 m	0.51	72 s
	25.0 m - 22.5 m	0.54	84 s
	22.5 m - 20.0 m	0.49	12 s
	20.0 m - 17.5 m	0.18	72 s
SR VI			
	32.5 m - 30.0 m	0.25	-120 s
	30.0 m - 27.5 m	0.40	-312 s
	27.5 m - 25.0 m	0.19	84 s
	25.0 m - 22.5 m	0.31	192 s

tuations at the upper swash-zone locations.

The single ebb-tide segment is more complicated (Figure 20). The maxima in crosscorrelation are at lags which suggest that the fluctuations are simutaneously migrating both down the foreshore and up the foreshore as shown by the elongation of the contours in an x-shaped pattern.

Crosscorrelation was also used to compare the runup data to the sediment level fluctuations. Problems were encountered as the result of the large difference in the periods of dominant motion. The dominant runup period was near 8 seconds, while the dominant sediment level oscillations had periods from 2 to 8 minutes. Low pass filtering of the runup records helped alleviate this problem. Figure 21 shows the low passed runup data along with the sediment level data for segment III. There are three obvious low frequency events in the runup time series that can be directly traced to the sediment level data. In all cases the best fit between the series occurs such that the lags show motions in the runup preceed the motions in the sediment level records. This would have to be the case if the runup is forcing the sediment level response. In general the crosscorrelation values are lower than those between adjacent stakes, and sensitive to the characteristics of

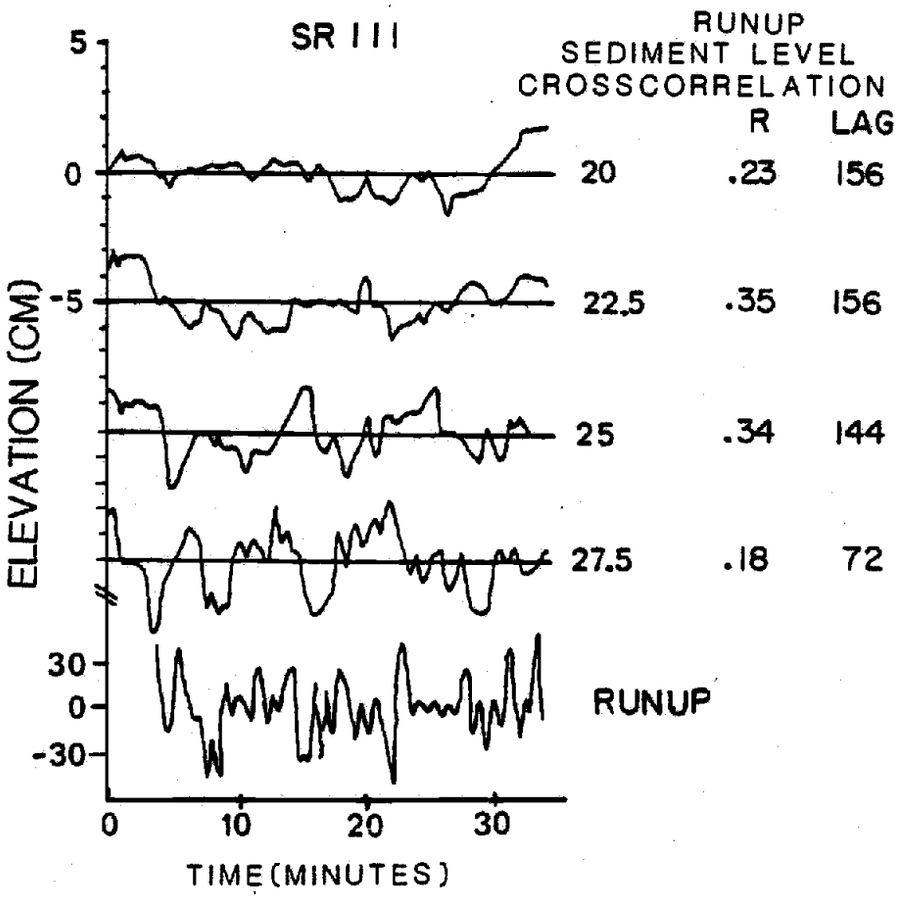

Figure 21. Detrended time series of sediment level and runup. The runup time series has been converted to a vertical excursion using the average foreshore profile and low pass filtered to exclude motions with periods of less than 70 s. The correspondence between the runup series and the sediment level time series at the seawardmost stake is obvious.

the filter applied to the runup time series. This is not surprising due to the assumed complexity of the transfer function between the runup and the profile response.

Spectral analysis was done to allow specific frequency bands to be examined and compared between simultaneous records. If direct forcing of the sediment level by the runup was occuring there should be peaks in the spectra at similar frequencies in both records. Due to the record length containing as few as three cycles of the sediment oscillations, and the fact that the sampling interval allowed resolution of only those periods greater than 100 seconds, the technique was of limited use. The results are subject to considerable error.

Figure 22 shows a series of sediment level spectra for the flood-tide segment on 21 October, 1982 (SR IV). This segment was 90 minutes in length. The sediment level records were detrended prior to the analysis. The sediment level spectra show a continuous decrease in energy in a landward direction. This was also noted by Sallenger and Richmond (in press). This trend held for all segments. In all cases the errors associated with the spectral estimates preclude making more specific comments on the analyses.

The cross spectra between the runup and sediment level were also subject to large error in order to maintain any

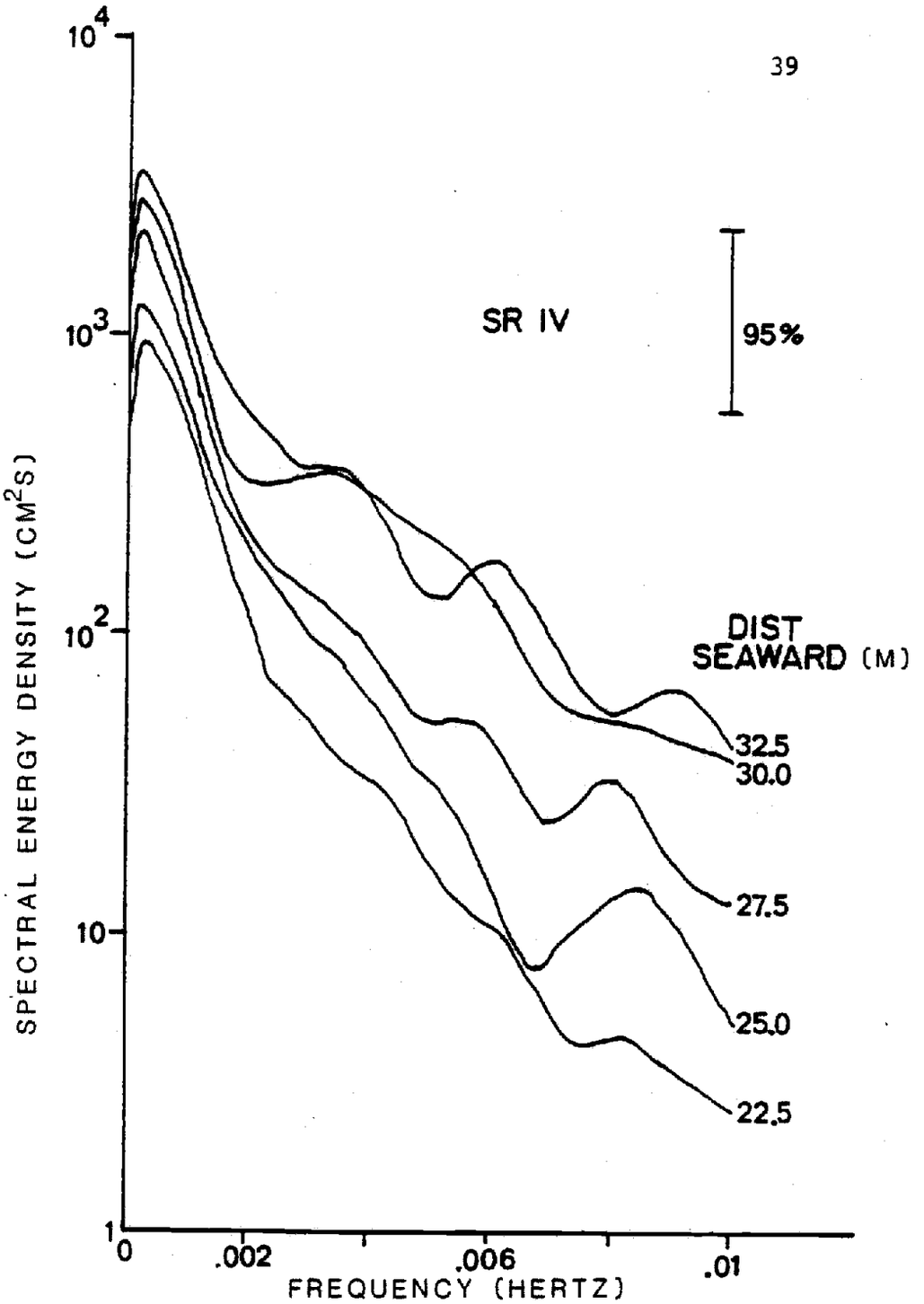

Figure 22. Sediment level spectra for time series of SR IV. There is a distinct trend for a decrease in energy at all frequencies for the landward stake locations. Peaks in the energy are not consistently located in specific frequency bands.

resolution of the peaks. Figure 23 shows the results of the cross spectrum between runup and stake 18 from SR I. The high values of coherence occur at the peaks in energy, and the associated phases indicate that the swash oscillations preceed the oscillations in sediment level.

Figure 24 shows a typical spectrum of runup. The distribution of energy is shown over a wider range of frequencies. As is typical for low wave conditions on a steep beach, the incident peak is clearly visible. Low frequency peaks are also present but at lower energy levels than the incident peak.

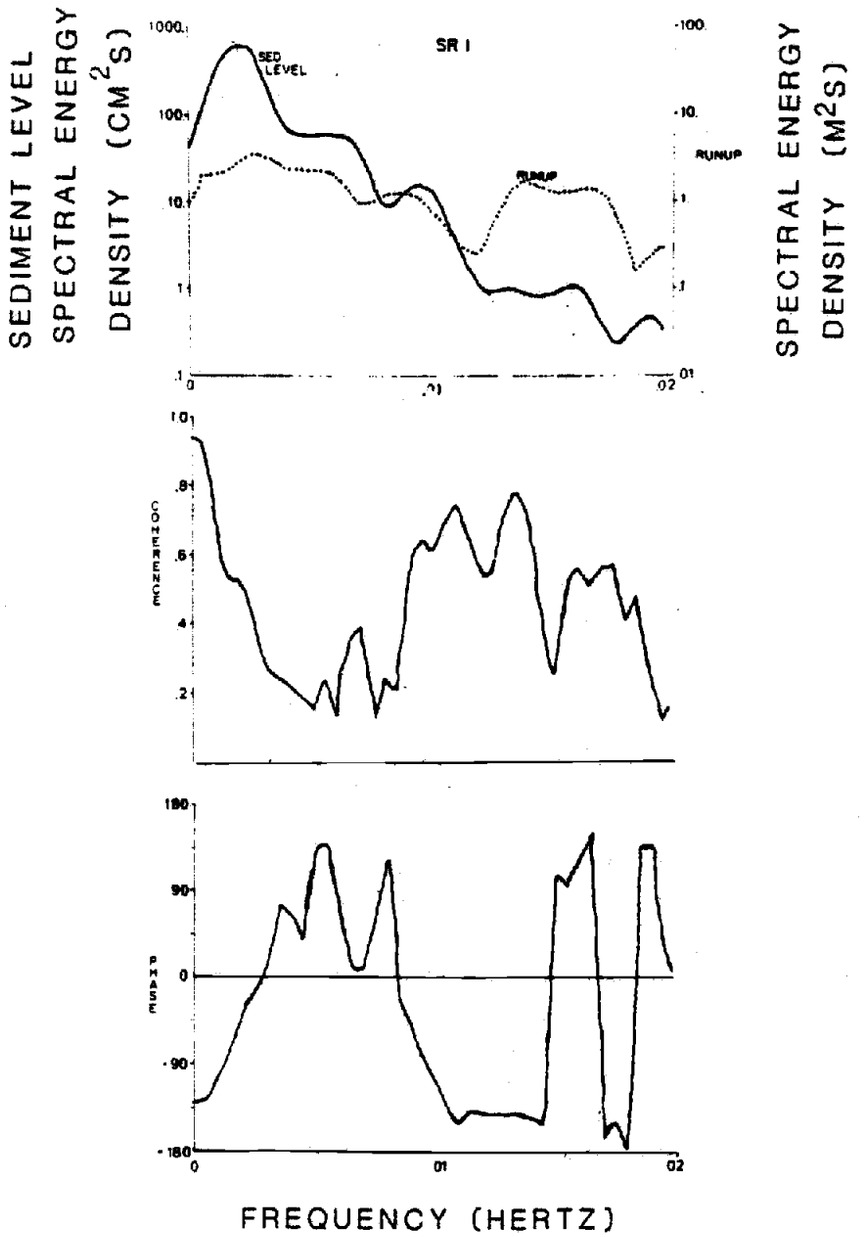

Figure 23. Cross spectrum between runup and sediment level for the stake at 18 m from SR I. While the peaks occur at similar frequencies, they are not coherent at the 90% level. These records provided the clearest results from the cross-spectral analysis. The 90% confidence limit for coherence is 0.73.

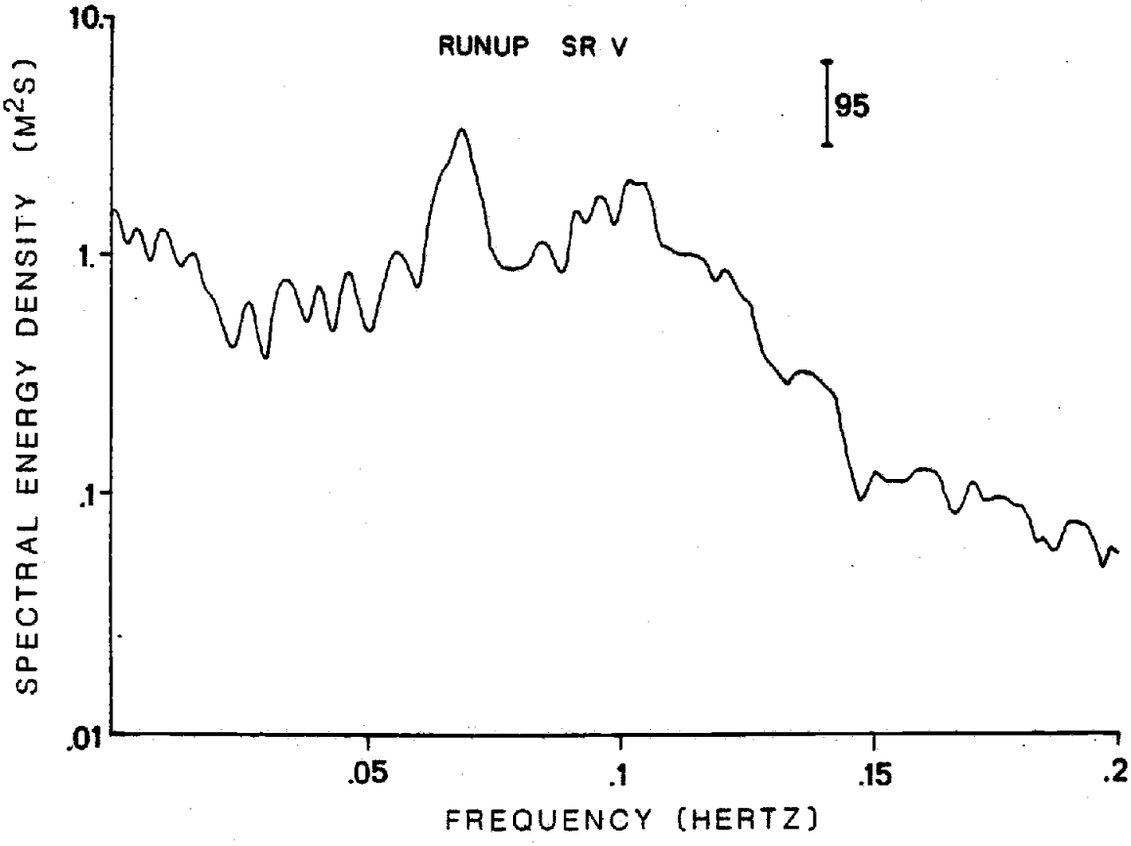

Figure 24. Runup spectrum, SR V. The spectrum shows the incident energy peak near a period of 8 seconds, a very strong subharmonic peak, and several smaller peaks at lower frequencies.

DISCUSSION OF FIELD DATA

Six data segments were collected on a high-energy, coarse-grained beach. Measurements of sediment level were made at a series of cross-shore locations on the foreshore at intervals of approximately 48 seconds. The record lengths ranged from 35 minutes to 90 minutes and the records covered different stages of the tide. In all cases high frequency (periods of 2 to 10 minutes) oscillations in sediment level with maximum heights of up to 6 cm were observed. Analyses of the records showed that for the most part the oscillations were progressing up the foreshore slope. In all cases there was a landward decrease in the RMS height of the oscillations. These trends were verified through the use of crosscorrelation analysis and spectral analysis.

There is some evidence to suggest that long period motions in the runup are responsible for the initiation of the observed sediment-level oscillations. The low frequency runup motions are correlated with the oscillations in sediment level and in all cases preceed in time the sediment level responses.

The sediment level fluctuations maintain their form despite the high energy of the swash-backwash action. This suggests that the forcing of the shape must be continued

past the initial formation of the features. The forcing must also occur below the zone of intermittant saturation. The occurence of the features below this zone does not conform with the hypothesis presented by Waddell (1976) and discussed earlier.

The data show that sediment level oscillations do occur on the foreshore of a beach in apparent response to long period waves. The origin of the waves is unknown, but recent work by Lanyon et al (1982) documents the shoaling of shelf waves with similar periods on beaches in Australia. The data confirm the two hypotheses, that long waves are capable of influencing the foreshore profile, and that the influence is not limited to the zone of intermittant saturation.

DYNAMICAL SIMULATION

To better understand the dynamics of the observed trends in the sediment level data, a numerical simulation model describing sediment transport on the foreshore was developed. In order to model the dynamics of the sediment level oscillations two things are needed, a model of sediment transport and a model of swash velocities.

Sediment Transport Model

The sediment transport model chosen was that of Bagnold (1963, 1966). This model has been applied to the surf-zone by Bowen (1980), Bailard and Inman (1981), and by Holman and Bowen (1983). Transport is assumed to be entirely suspended load. The foreshore slope is assumed to be composed of an equilibrium component and a perturbation component. The equilibrium component is in balance with the runup velocity, composed of the velocities of the incident waves and any long term net flows. The perturbation slope is in response to perturbations in the runup velocity field. The sediment transport equation will be simplified to relate the perturbation transport to the perturbation slope and to the time-averaged swash velocity.

Depth-integrated immersed-weight suspended load transport is given by the equation (Bagnold, 1963)

$$i_s(x,t) = \frac{\epsilon_s C_d \rho}{w} U^3 |U| \left(1 - \frac{\beta U}{w}\right)^{-1} \tag{1}$$

where ϵ_s is an efficiency, C_d is a drag coefficient, ρ is the water density, w is the fall velocity of the sediment, U is the total velocity of the flow, and the quadratic drag law is assumed to be valid. Converting this to volume transport gives

$$q_s = \frac{\epsilon_s C_d \rho}{(\rho_s - \rho) g w} U^3 |U| \left(1 - \frac{\beta U}{w}\right)^{-1} \tag{2}$$

where ρ_s is the sediment density and g is the acceleration due to gravity. Time and space dependence of the transport is assumed throughout the analysis.

Total velocity, U, may be written as

$$U(x,t) = u_o(x,t) + u_1(x,t) \qquad u_o(x,t) >> u_1(x,t) \tag{3}$$

where u_o is the velocity contributed by the runup of the incident gravity wave field and u_1 is the sum of any drift velocities present. The beach slope is assumed to be composed of two terms,

$$\beta(x,t) = \beta_o(x,t) + \beta'(x,t) \tag{4}$$

where $\beta_o(x)$ is the equilibrium slope and $\beta'(x)$ is a perturbation slope resulting from disequilibrium. Figure 25 defines the coordinate system used, x being positive seaward, z positive up, and the depth, h, the location of the sediment surface, is defined as $h(x,t) = -z$.

If we assume that the autosuspension criterion is not exceeded, that is

$$\frac{\beta U}{w} < 1 \tag{5}$$

then the transport may be approximated by substituting (3) and (4) as

$$q_s = \frac{\epsilon_s C_d \rho}{(\rho_s-\rho)gw} (u_o+u_1)^3 \left|u_o+u_1\right| \left(1 - \frac{(\beta_o+\beta')(u_o+u_1)}{w}\right)^{-1} \tag{6}$$

This equation may be expanded to give the result

$$q_s = \frac{\epsilon_s C_d \rho}{(\rho_s-\rho)gw} \left[u_o^3\left|u_o\right| + u_o^4\left|u_o\right|\frac{\beta_o}{w} + 4u_1u_o^2\left|u_o\right| + \right.$$

$$\left. 5u_1u_o^3\left|u_o\right|\frac{\beta_o}{w} + u_o^4\left|u_o\right|\frac{\beta'}{w} + \cdots\right] \tag{7}$$

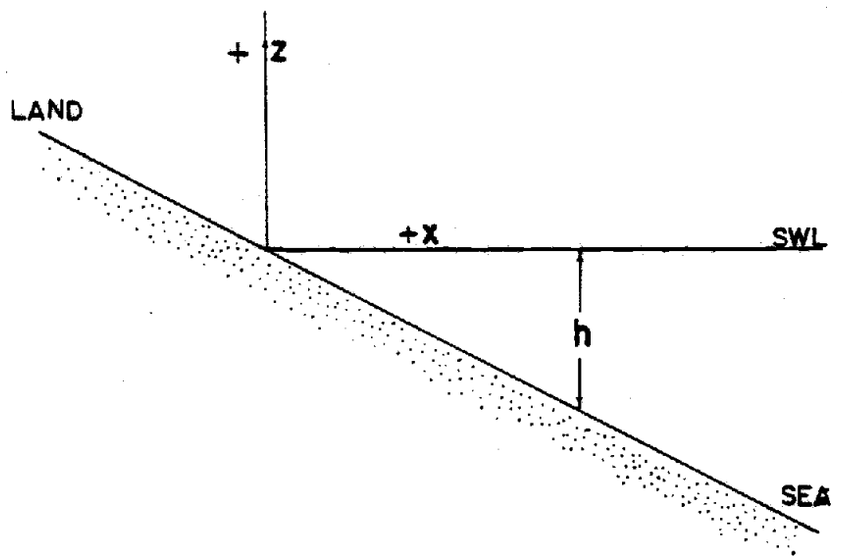

Figure 25. Definition sketch. The axes are defined with x positive seaward and z positive up. The depth of the sediment surface, h, is equal to -z, or positive down.

ignoring terms of the order β'^2, $\beta' u_1$, or u_1^2 and higher.

By definition, the equilibrium slope, $\beta_o(x)$, is in equilibrium with the velocity terms, thus the time averaged transport associated with these terms is zero, or

$$\langle q_{s\ eq} \rangle = \langle u_o^3 | u_o | \rangle + \langle u_o^4 | u_o | \frac{\beta_o}{w} \rangle +$$

$$\langle 4u_1 u_o^2 | u_o | \rangle + \langle 5u_1 u_o^3 | u_o | \frac{\beta_o}{w} \rangle + \cdots = 0 \qquad (8)$$

where $\langle \ldots \rangle$ denotes time averaging. Substituting leaves the time-averaged perturbation transport terms

$$\langle q_s' \rangle = \frac{\epsilon_s C_d \rho}{(\rho_s - \rho) g w} \left(\langle u_o^4 | u_o | \rangle \frac{\beta'}{w} + \cdots \right) \qquad (9)$$

Gradients in this perturbation transport will alter the perturbation beach profile, $h'(x)$. These changes can be calculated through the continuity equation where P is the void ratio of the deposited sediment:

$$\frac{\partial h'}{\partial t} - \frac{1}{(1-P)} \frac{\partial \langle q_s' \rangle}{\partial x} = 0 \qquad (10)$$

Substituting and keeping only the most significant terms gives

$$\frac{\partial h'}{\partial t} = \frac{1}{(1-P)} \frac{\epsilon_s C_d \rho}{(\rho_s-\rho)gw^2} \left(\beta' \frac{\partial}{\partial x} \langle u_o^4 | u_o | \rangle + \langle u_o^4 | u_o | \rangle \frac{\partial \beta'}{\partial x}\right) \quad (11)$$

assuming that there are gradients only in the time-averaged velocity and β'.

The assumption of suspended load transport is not without merit. Bowen (1980) gives the ratio of the suspended transport terms to the bedload transport terms as

$$\frac{1}{15} \frac{U_{max}}{w} \quad (12)$$

for the assymmetry terms of flow and as

$$\frac{1}{15} \tan \phi \left(\frac{U_{max}}{w}\right)^2 \quad (13)$$

for the gravitational terms. These ratios, where U_{max} is the maximum swash velocity and ϕ is the angle of repose, give ratios of 3.33 and 100.0 for the importance of suspended load relative to bedload when w is 0.1 m/s and U_{max} is 4.5 m/s. In any case, the solution for bedload transport (Bagnold, 1963) results in an equation for the time-averaged perturbation transport of the same form as equation 9, but to a lower power of velocity

$$\langle q_b'(x,t)\rangle = \frac{\epsilon_b C_d \rho}{(\rho_s-\rho)g \tan^2\phi} \langle u_o^2 | u_o | \rangle \beta' \qquad (14)$$

where ϵ_b is an efficiency associated with bedload transport. This implies that the physics governing the processes will be the same under any assumption regarding the mode of transport. In either case, the perturbation will progress landward. However, since bedload transport is independent of w, there would be no relationship between grain size and the rate of migration if bedload transport were assumed.

Runup Velocity Model

Models of runup velocities and distances have been reported previously. Shen and Meyer (1963) used the method of characteristics to find the equation which describes the position of the leading edge of the runup:

$$x(t) = -u_i t + \tfrac{1}{2} g \beta t^2 \qquad (15)$$

where u_i is the initial velocity. The velocity of the leading edge is then:

$$u(t) = -u_i + g\beta t \qquad (16)$$

These equations yield constant acceleration of the runup front due to gravity and thus a parabolic relationship between distance and time.

Hibberd and Peregrine (1979) expanded upon this work and solved for the internal flow. They used Shen and Meyer's (1963) solution for the leading edge as a bound for their work. Their results allowed for the formation of a backwash bore. This possibility is not included in the model adopted below.

For the purposes of this work the swash velocity and distance relationships with time were taken as being dependent on friction, f, gravity, g, and the beach slope, β:

$$\frac{\partial u}{\partial t} = g\beta - fu \tag{17}$$

This equation can be solved to give

$$u(t) = \frac{g\beta}{f} - \frac{C}{f} e^{-ft} \tag{18}$$

where C is a constant. Boundary conditions are then applied such that at t = 0 the velocity is equal to the initial velocity

$$u = -u_i \quad \text{at } t = 0 \tag{19}$$

which implies that

$$C = g\beta + fu_i \tag{20}$$

The runup is also assumed to be periodic and to return to $x = 0$ in one swash period, T:

$$x = 0 \quad \text{at } t = 0 \tag{21}$$

$$x = 0 \quad \text{at } t = T \tag{22}$$

Making the appropriate substitutions and solving for u(t) and x(t) gives

$$u(t) = \frac{g\beta}{f} - \frac{g\beta T}{(1-e^{-fT})} e^{-ft} \tag{23}$$

and

$$x(t) = \frac{g\beta t}{f} - \frac{g\beta T}{f} \frac{(1-e^{-ft})}{(1-e^{-fT})} \tag{24}$$

Implicit in the formulation of this model is an assumption that should be pointed out. There are no terms included in equation 17 that describe pressure gradients or the advection of momentum. This assumption results in a runup mass of uniform depth (with a discontinuity at the front) and with no internal velocity gradients. Figure 26

gives a depiction of the runup. Specifing the runup in this manner precludes solving for time- or space-varying runup depth. Velocity is allowed to vary only in time. These assumptions allow for a more simple sediment transport calculation scheme to be employed.

This model for runup velocity and distance is sensitive to the values used for beach slope and runup period. Figures 27 through 32 show the dependencies for a wide range of values for f, T, and β. For given values of T and f (Figures 27 and 28) an increase in slope will result in a higher initial velocity and thus a greater value for the maximum runup distance. An increase in period with constant slope and friction (Figures 29 and 30) will also have the effect of increasing the initial velocity of the runup and thus the maximum excursion. Friction has little effect on the initial velocity or on the maximum runup. It does provide a slight landward assymmetry to the time averaged flow. The effects of friction are shown in Figures 31 and 32.

Several comparisons between theory and actual data have been made. Waddell (1973) reported that his field data of runup on a natural beach agreed with the values predicted by Shen and Meyer (1963) to within "30% and most often within 15%." He compared the predicted duration of

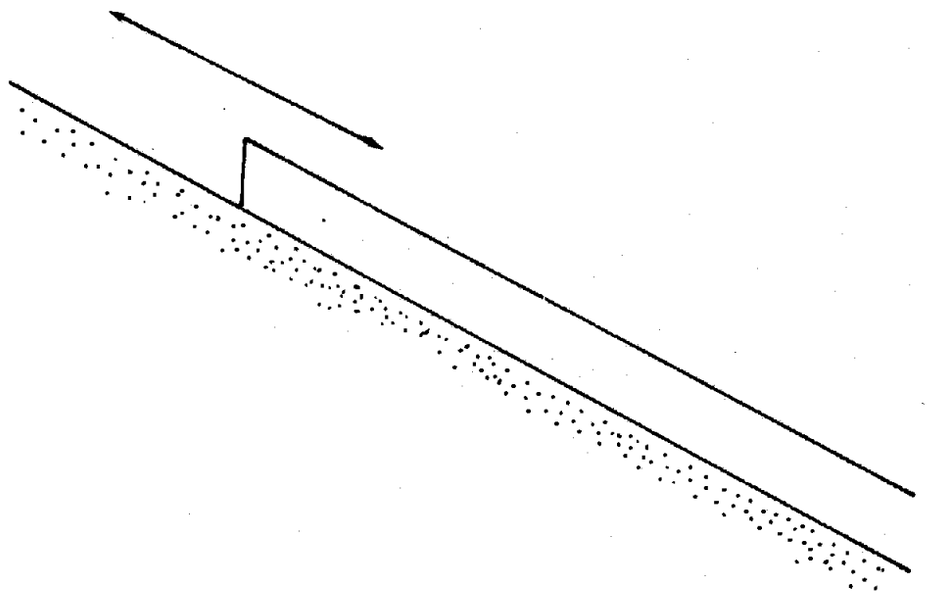

Figure 26. Runup under the assumptions of the model. The runup is of constant depth in time and space. The runup velocity varies only in time.

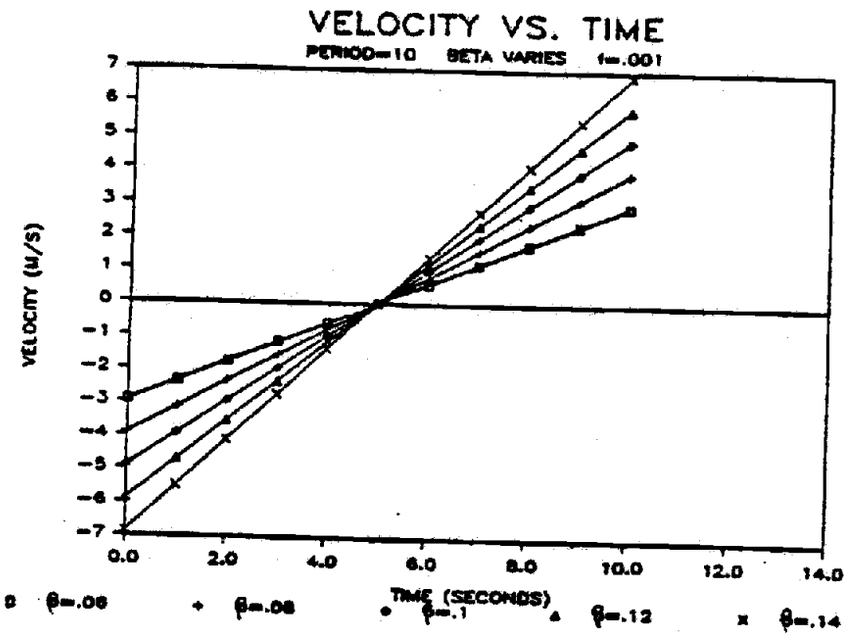

Figure 27. Velocity versus time as predicted by the model for a range of beach slope values. As the slope increases, higher initial and final velocities result if friction and period are held constant.

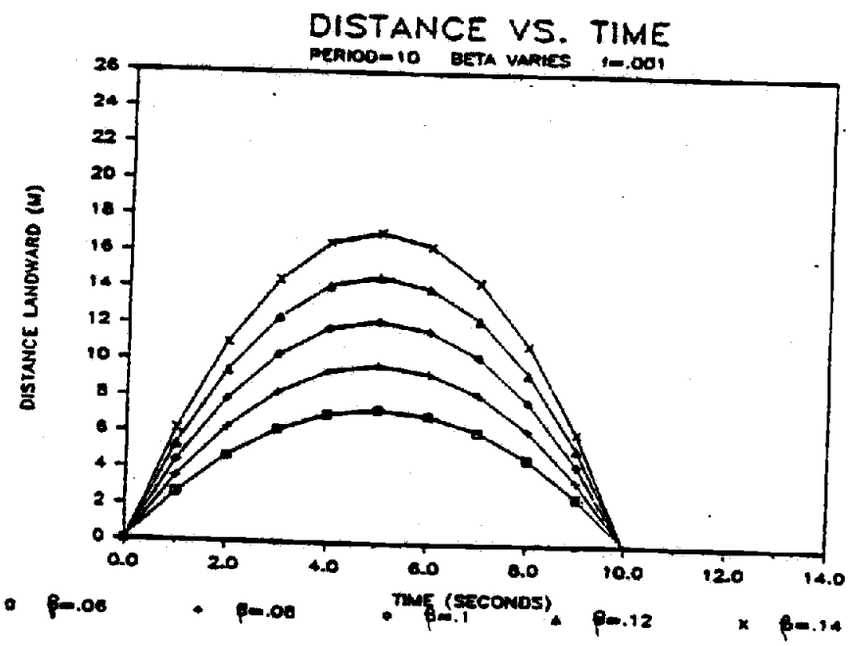

Figure 28. Distance versus time for a series of beach slopes with constant friction and period. A larger beach slope results in a larger maximum excursion.

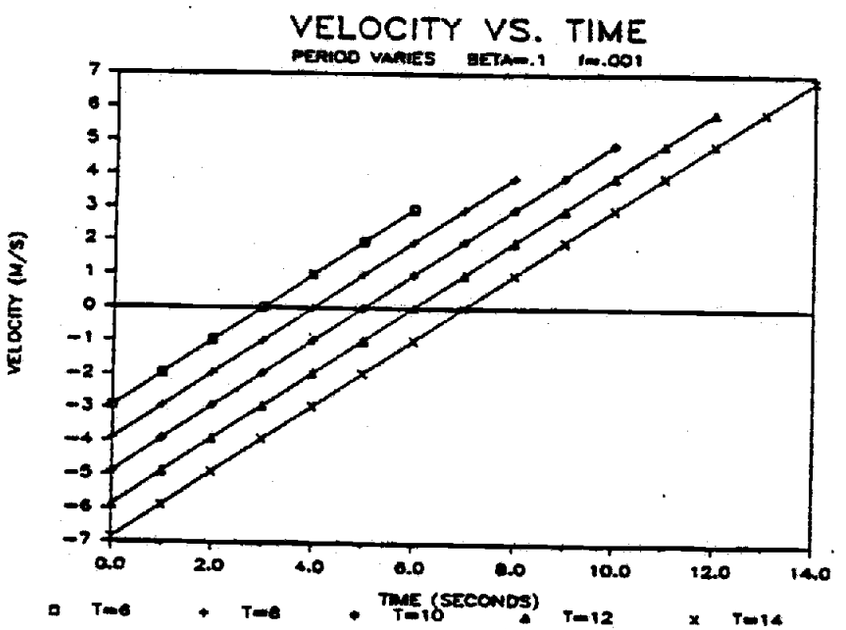

Figure 29. Velocity versus time for a series of values for the period. Larger periods result in higher initial and final velocities.

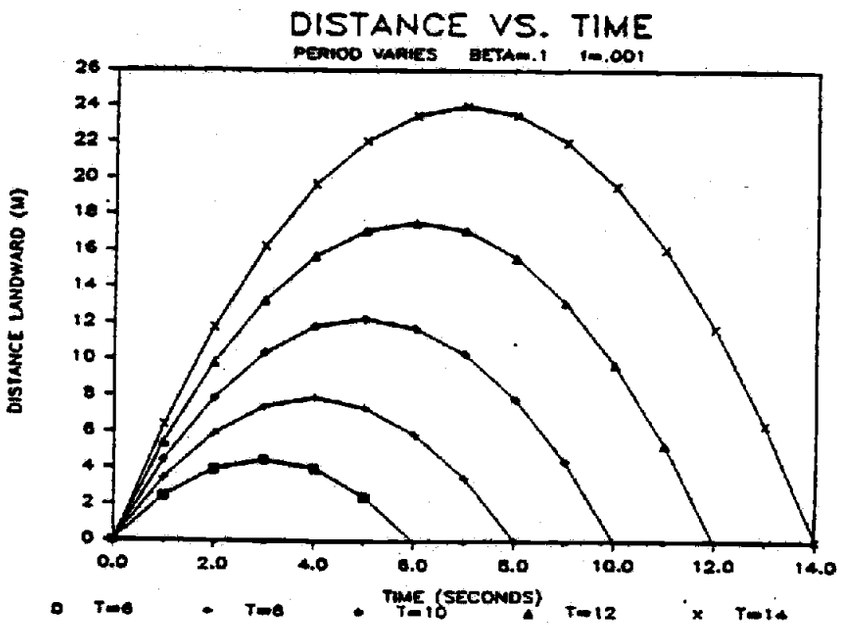

Figure 30. Distance versus time for a series of periods. Larger periods result in larger runup excursion.

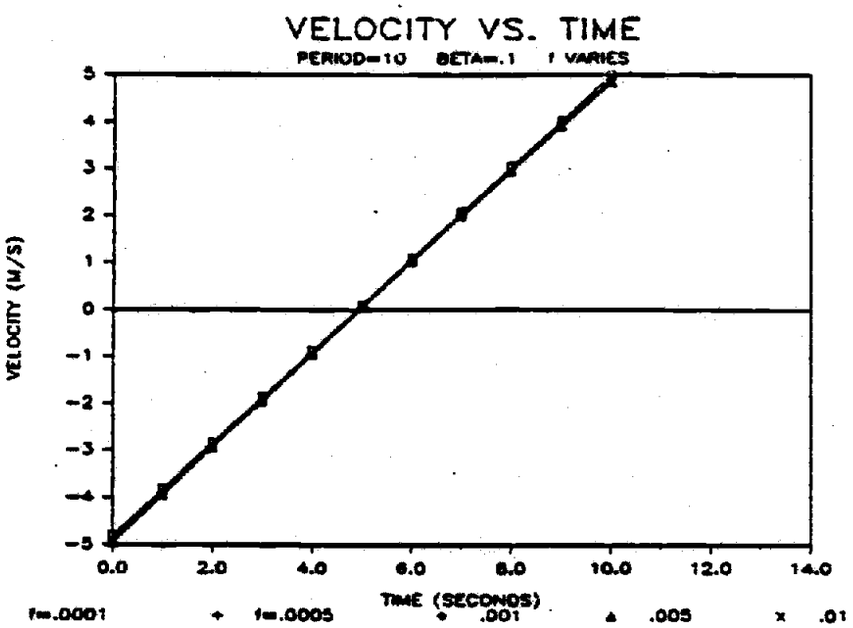

Figure 31. Velocity versus time for a range of values for friction. There is little effect over the two orders of magnitude shown.

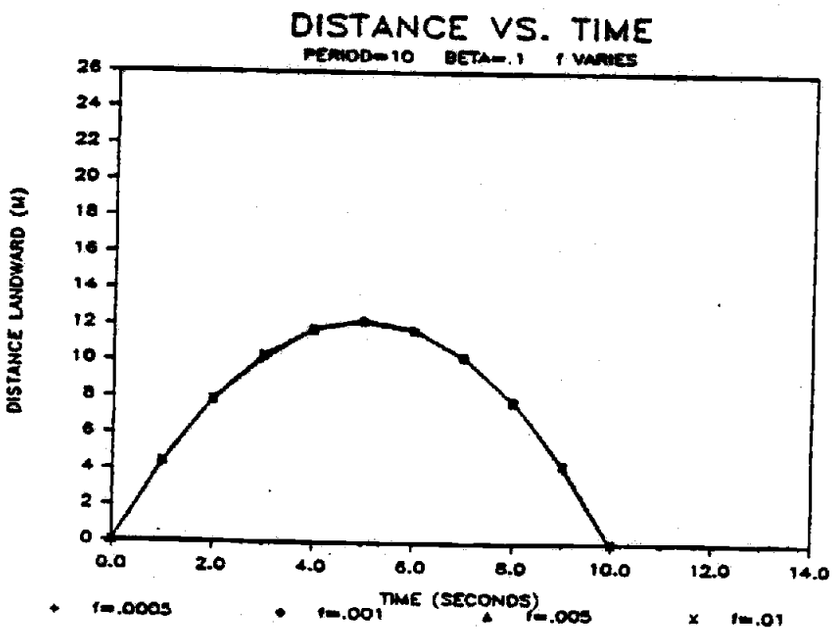

Figure 32. Distance versus time for different values of friction. There is little effect.

submergence of a location with that actually observed. This is a test of the equation Shen and Meyer (1963) used for determining the location of the leading edge of the upwash and the trailing edge of the backwash. This suggests that the parabolic relationship between distance and time is valid as a first order approximation.

Miller (1968) compared theoretical solutions for runup with data from a laboratory study. He concluded that the runup excursion could be predicted, but that the slope of the beach and friction must be included in the solution. He also noted an inflection point in the runup velocity curves in the area where there is a transition from the incident wave to the runup. His data show that for the case of a fully developed bore the transition zone from bore to runup occurs very near the intersection of the still water line and the beach face. Once transformed to runup the velocity decreased linearly with time for all cases. The model of runup presented earlier also predicts a linear change in velocity with time.

To further test the validity of the model, runup data obtained on 21 October 1982 during collection of sediment level data were analyzed. Figure 33 presents a plot of runup velocity versus non-dimensional time for a series of waves. Time was normalized by the length of time be-

tween the beginning of each swash, essentially the runup period. The swash of each wave ($u < 0$) and the beginning of the backwash show constant acceleration with time. The end of the backwash phase does not. This is primarily due to the interaction of the backwash of a wave with the swash of the next. Figure 34 shows a time series of three successive runup events. The parabolic nature of the swash phase of the runup is quite evident. The backwash shows less of a parabolic nature. This may be the result of the digitization of the film records as well as actual physical processes. It is quite easy to follow the leading edge of the swash, but the location of the trailing edge of the backwash is often difficult to determine. The interactions of the swash and backwash are evident from the fact that wave two begins to move landward prior to wave one returning to its point of origin. The runup model assumed that there was no such interaction between a swash and the preceeding backwash.

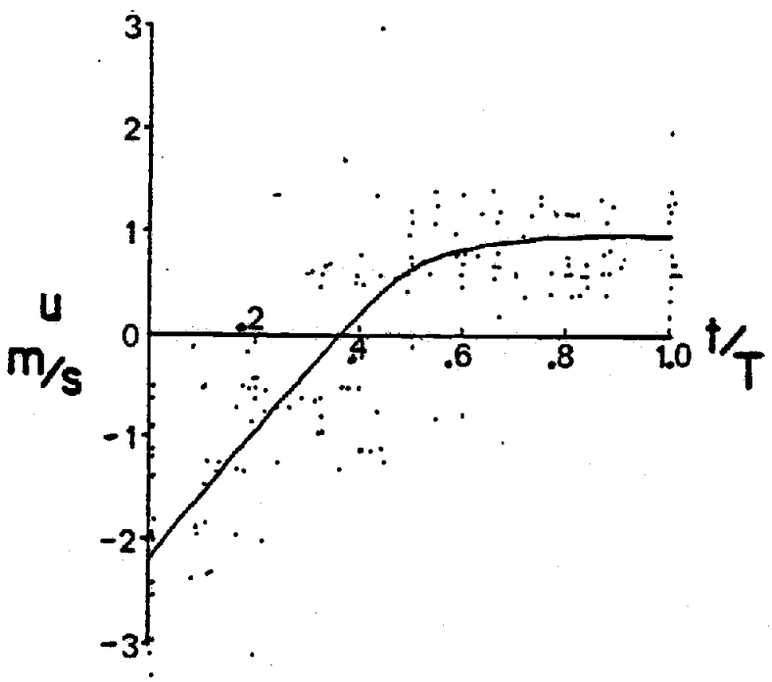

Figure 33. Runup velocity versus dimensionless time for a series of waves measured on 21 October 1982. Time was normalized for each runup by its period. The data show a constant acceleration throughout the swash and the first half of the backwash. Swash-backwash interactions then interfere. The runup model included no provision for these interactions.

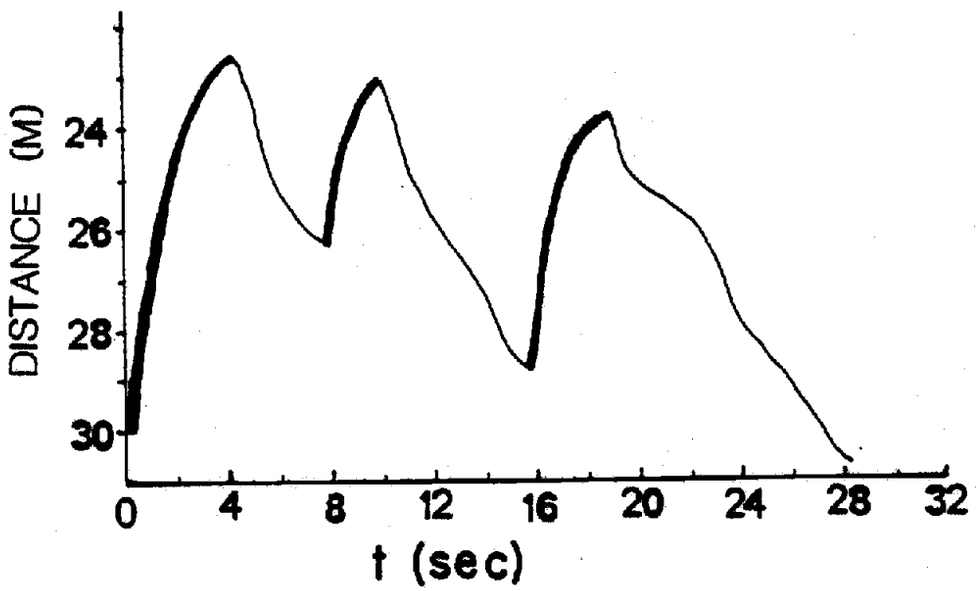

Figure 34. A time series of three consecutive runup crests recorded 21 October 1982. The swash of each follows a parabolic path. The backwash phase does not seem to do so. The interaction of the swash with the preceeding backwash may be the cause. Problems associated with the film digitization technique may also cause this.

DYNAMICAL MODEL RESULTS

Figures 35 to 37 show the results of the model for fall velocities of 0.05 m/s, 0.075 m/s, and 0.1 m/s, chosen as representative of the grain sizes present (Baba and Komar, 1981). In each case the values for C_d, ϵ_s, and the densities of the fluid and the sediment were constant. The value of ϵ_s was taken to be 0.01 as suggested by Bagnold (1966). C_d was assigned the value 0.001. The densities were taken to be 1.025 g/cm^3 for the seawater and as 2.65 g/cm^3 for the sediment. The time-averaged velocity profile was calculated based on a foreshore slope of 0.1, a swash period of 10 s, and a friction coefficient of 0.001. In each figure there is no change in the grain size on the beach foreshore, the change occurs between successive figures. It is clear that the perturbation migrates landward and decreases in amplitude for all values of fall velocity. The migration is most rapid for small values of w (small grain size). The rate of migration slows as the perturbation progresses landward. Figure 38 gives an additional picture of perturbation migration for a negative original perturbation. Note that in all cases the perturbation migrates landward at a decreasing rate and that the amplitude decreases as well. The migration of the perturbation has no effect on the profile; there is no net

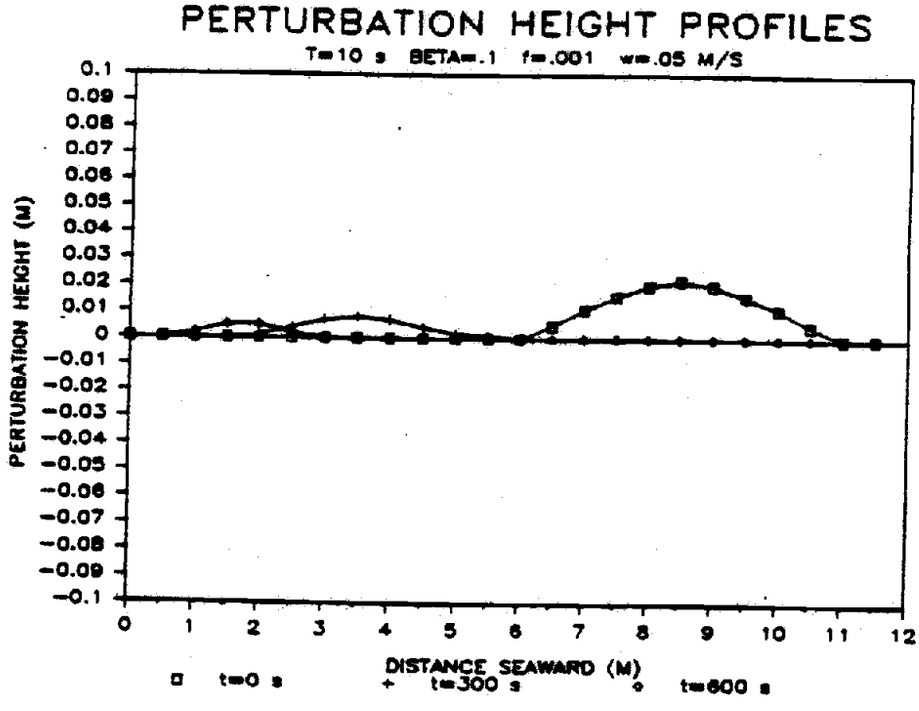

Figure 35. Perturbation height profiles, w = 0.05 m/s. Model results for a velocity field determined for a beach slope of 0.1 and a period of 10 s. Fall velocity of the sediment was taken as 0.05 m/s. The initial perturbation progressed landward and decreased in amplitude. The rate of migration slowed landward. Note that the migration does not result in net erosion or deposition. Run length is 600 seconds.

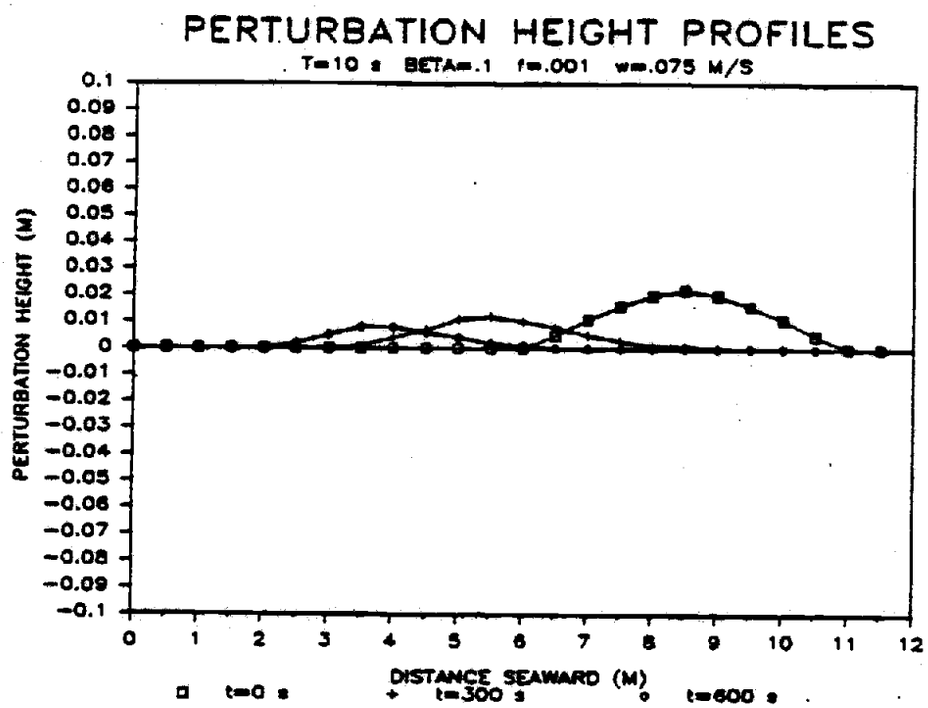

Figure 36. Perturbation height profiles, w = 0.075 m/s. The perturbation migrated landward more slowly than was the case for w = 0.05 m/s. Note that the passage of the perturbation does not result in any net change in the profile.

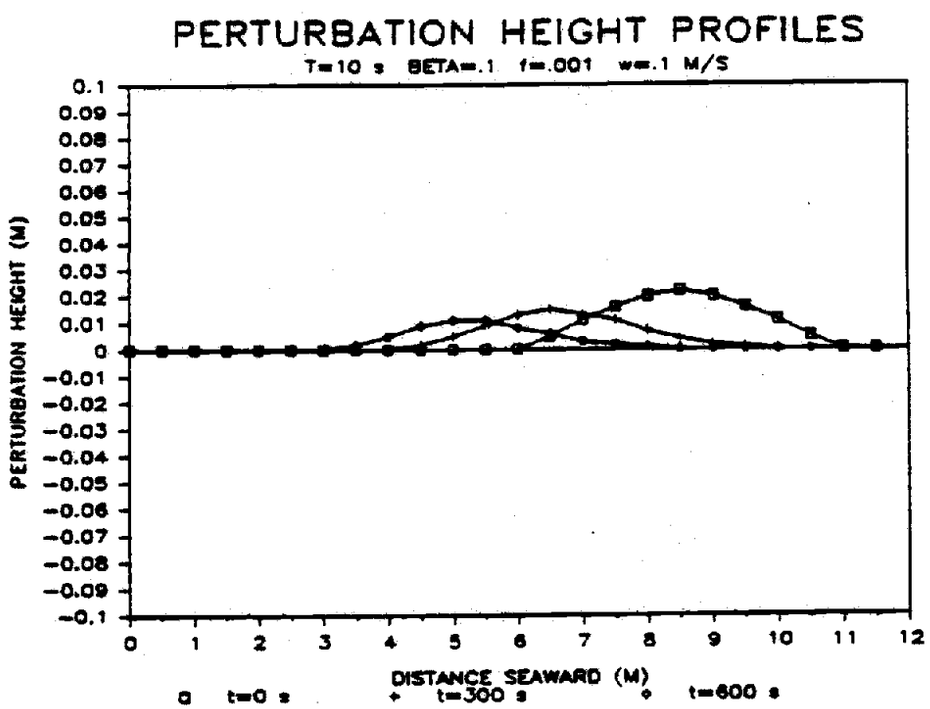

Figure 37. Perturbation height profiles, w = 0.1 m/s. The perturbation progresses up the foreshore, and makes no contribution to the net sedimentation of the locations it passes. The landward decrease in height is not as obvious in this case.

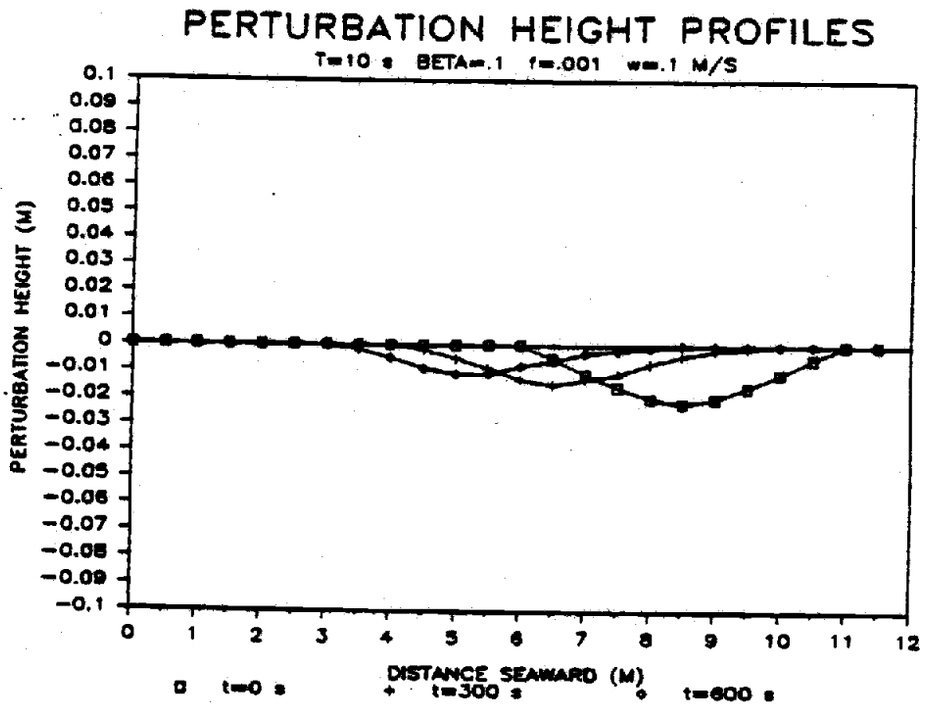

Figure 38. The migration of an initially negative perturbation. The form decreases in amplitude, progresses landward, and results in no net change in sediment level.

erosion or deposition.

In all cases migration results from the term

$$\beta' \frac{\partial \langle u_o^4 | u_o | \rangle}{\partial x}$$

in equation 11. Figure 40 shows the influence of this term alone. Sediment is deposited on slopes which are less than β_o and eroded on those slopes greater than β_o. The perturbations steepen during migration due to the fact that the erosion (or deposition) occuring seaward of the crest (or trough) of the perturbation is occuring at a more rapid rate than the deposition (erosion) on the landward flank. Sallenger and Richmond (in press) noted that the perturbations they measured migrated in response to the erosion on the seaward flank of the perturbation exceeding the rate of deposition on the landward flank. This is also the case for the perturbations measured in this study.

Figure 41 shows the results of considering the term

$$\langle u_o^4 | u_o | \rangle \frac{\partial \beta'}{\partial x}$$

from equation 11. The effect of this term is to smooth the original perturbation. Deposition occurs where the β' gradient is negative and erosion occurs where it is

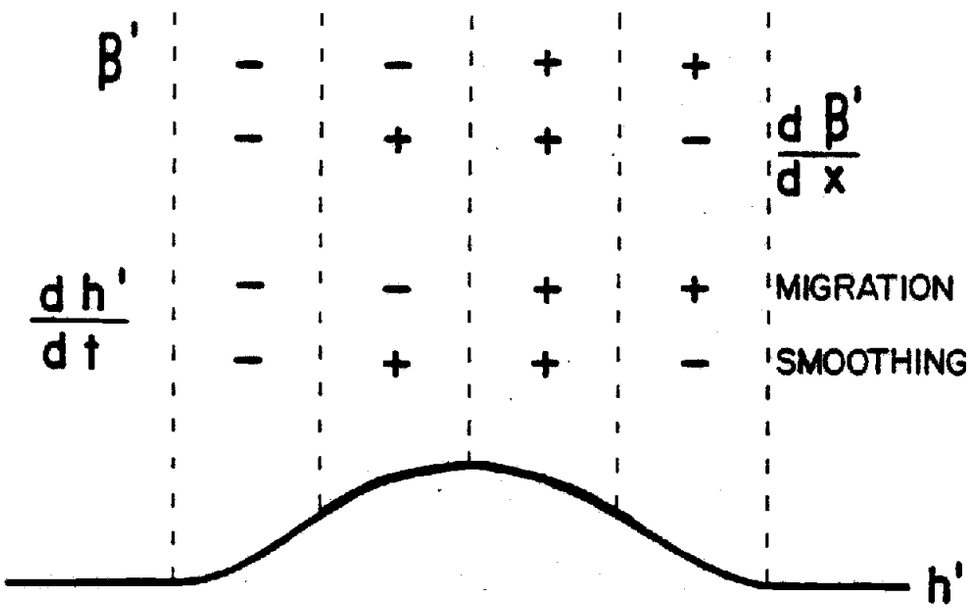

Figure 39. Zones of erosion and deposition. The model predicts that erosion will occur where the total slope exceeds the equilibrium slope (the perturbation slope is positive) and where the derivative of the perturbation slope is positive. Deposition is predicted where those terms are negative. Remember that h, the depth to the sediment surface, increases as erosion occurs.

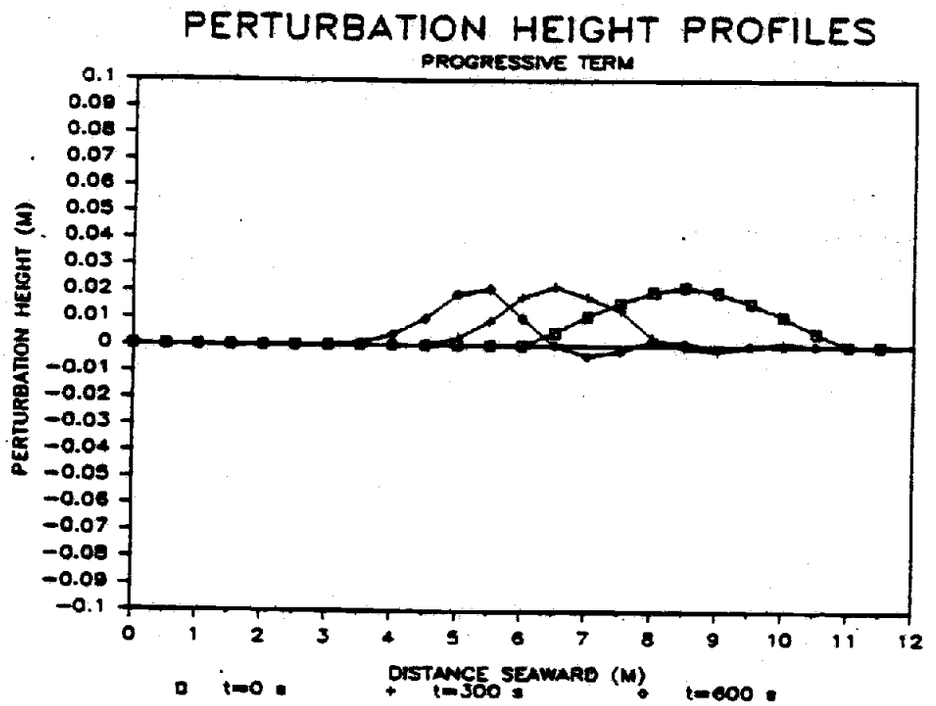

Figure 40. The results from considering the progressive term alone. Progression occurs with erosion on the seaward flank and deposition on the landward flank. The perturbation steepens and does not decrease in height.

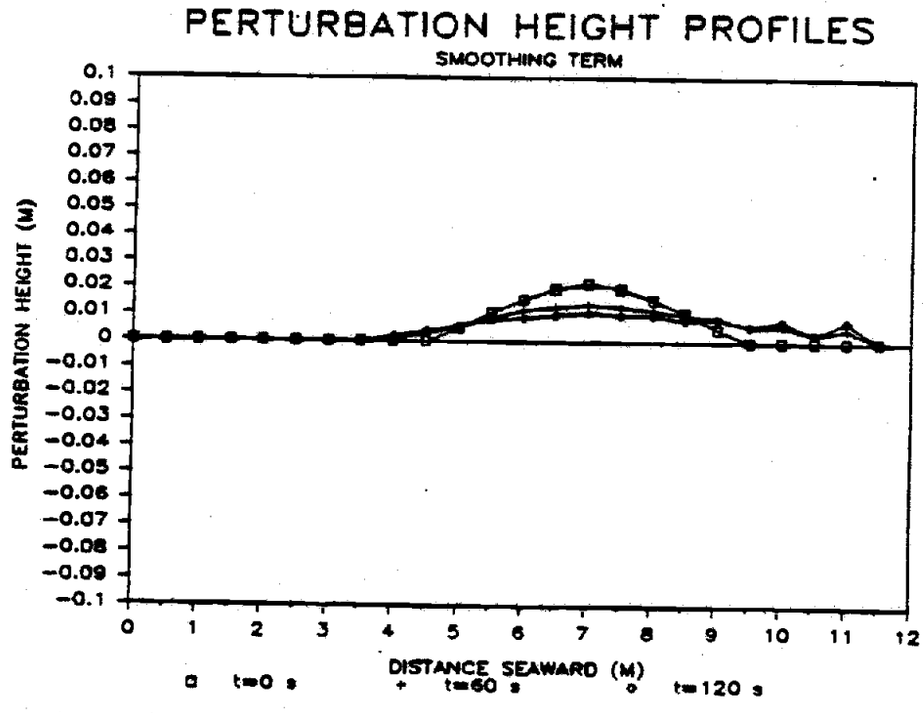

Figure 41. The results from considering the smoothing term alone. The form rapidly decreases in height due to erosion where the β' gradient is positive and dep-deposition where negative.

positive. This smoothing is very rapid. Note that the original perturbation is decreased to half its height in 120 seconds in the case presented.

Due to the rapidity with which the smoothing takes place, this term was scaled by a factor of 0.1 in producing the results shown in Figures 35 to 38. The scaling factor was arbitrary, but represents the continued forcing of the perturbation shape during migration. The nature of the forcing is discussed later.

Trends in the velocity of migration of the fluctuations can be derived from equation 11 as well. For the simple case of a perturbation with slopes of constant β' and a flat top, the velocity of migration can be shown to be dependant on the magnitude of the time averaged velocity gradient. Figure 42 defines the symbols used below. The progressive term of equation 11 gives the relationship

$$\frac{\partial h'}{\partial t} = \frac{1}{(1-P)} \frac{\epsilon_s C_d \rho}{(\rho_s-\rho)gw^2} \left(\beta' \frac{\partial}{\partial x} \langle u_o^4 | u_o | \rangle\right) \qquad (25)$$

For any point on the landward slope, the crest of the perturbation will have progressed $\Delta x = x^* = -\frac{h^*}{\beta'}$ when the profile has risen $\Delta h' = h^*$. From the above equation, the time taken for the progression will be

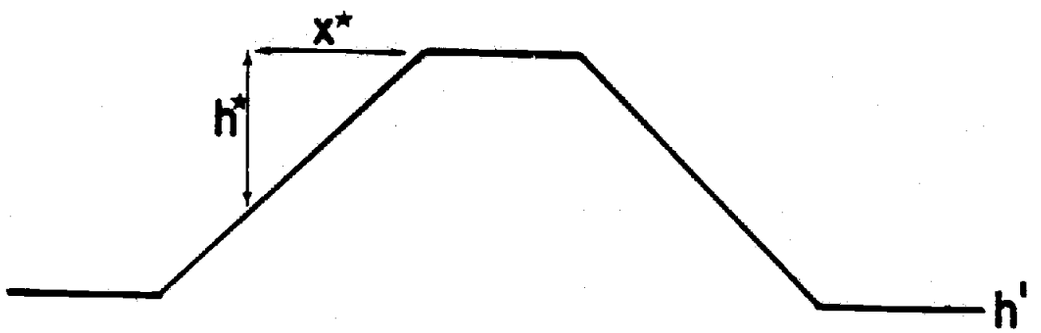

Figure 42. Definition sketch for the derivation of the rate of migration of the perturbations. Starred quantities, h^* and x^*, refer to the height and distance gained during progression.

$$\Delta t = \frac{h^*}{\frac{1}{(1-P)} \frac{\epsilon_s C_d \rho}{(\rho_s-\rho)gw^2}(\beta' \frac{\partial}{\partial x}\langle u_o^4 | u_o | \rangle)} \tag{26}$$

and the velocity of the progression, C_p, will be

$$C_p = -\frac{1}{(1-P)} \frac{\epsilon_s C_d \rho}{(\rho_s-\rho)gw^2}(\frac{\partial}{\partial x}\langle u_o^4 | u_o | \rangle) \tag{27}$$

Progression will always be landward for cases where the time-averaged velocity gradient is positive.

Since the rate of migration of the perturbations is inversely related to w^2, any change in the grain size on the foreshore will result in predictable changes in the migration velocity. An increase in the grain size at any location ($\frac{\partial w}{\partial t} > 0$) on the foreshore over time will result in an apparent shift toward a lower frequency of oscillation at that location. Similarly, a constant spacial gradient ($\frac{\partial w}{\partial x}$ = constant) in grain size on the foreshore will cause changes in the rate of migration but would not produce frequency shifts, since the travel time of each oscillation would remain the same, as would the time between arrivals.

DISCUSSION

This study has shown that rapid sediment level oscillation do occur on the foreshore of coarse-grained beaches. The zone of their occurence corresponds with that discussed by Sallenger and Richmond (in press) and extends the zone reported by Waddell (1973, 1976). Crosscorrelation analysis shows that in most cases the oscillations progress landward. The RMS heights of the oscillations decrease in a landward direction. The relationship between the sediment level records and low-passed runup records suggests that the oscillations in the sediment level are being forced by low frequency waves.

The fact that the oscillations are present on all sections of the foreshore subject to swash action discounts the hypothesis presented by Waddell (1976) for the origin of these features. He stated that the oscillations were the result of periodic saturation and unsaturation of the foreshore. According to Waddell (1976), unsaturated foreshore resulted in the deposition of sediment while later saturation resulted in erosion. The change in the saturation state was hypothesized to result from long period waves in the inner surf-zone. If Waddell's (1976) hypothesis were true, then on a foreshore of the steepness of the

beach studied here, the long period wave would need to have an amplitude of greater than 1 m in order to force fluctuations of the saturation line that would extend over the range required. There was no evidence that such high-amplitude, low-frequency waves existed at the time of the study. The oscillations were also measured seaward of the lowest position of the saturation line. It should be noted that the beach on which Waddell did his study was of considerably lesser slope and a wave of smaller amplitude would be required.

The simulation model, which has been shown to provide an adequate representation of the migration and decay of the oscillations, may also shed some light on the original formation of the perturbations.

The step-zone of the foreshore is a common feature of many steep beaches. It is a zone characterized by the steepest slopes found on the beach, often near the angle of repose (Wright et al, 1979). Sallenger (personal communication) noted that in one experiment they extended their measurements to locations seaward of the step and that no oscillations were present in those records. This would suggest that the oscillations are generated in the lowermost foreshore near the vicinity of the step.

If the slopes associated with this zone were to be

temporarily thrown out of equilibrium by a long-period wave of sufficient magnitude and duration for a response, the model presented earlier would predict deposition landward of the step where the slope is suddenly much too flat and erosion on the face of the step itself. If the long wave is at a period allowing insufficient time for equilibrium to be reached, a perturbation in the foreshore profile is the result. Forcing of the perturbation shape will continue until equilibrium is reached. If the rate of rise does not allow equilibrium, the forcing may counteract the tendency of the beach to smooth itself. Figure 43 summarizes this conceptual explanation for the formation of the perturbations.

An alternative explanation for the formation of the sediment-level oscillations is the formation of antidunes in the lower swash-zone. Antidunes form in supercritical flow, such as may occur during the latter stages of backwash. The migration of the form as an antidune is dependent on maintaining supercritical flow above the bedform. This could not be the case in the upper swash-zone. Furthermore, the direction of antidune migration is opposite to the direction of sediment transport. The observed oscillations migrate landward regardless of the direction of net sediment transport. So while antidunes may explain the

initial formation of the oscillation, they do not explain the migration of the form on the foreshore.

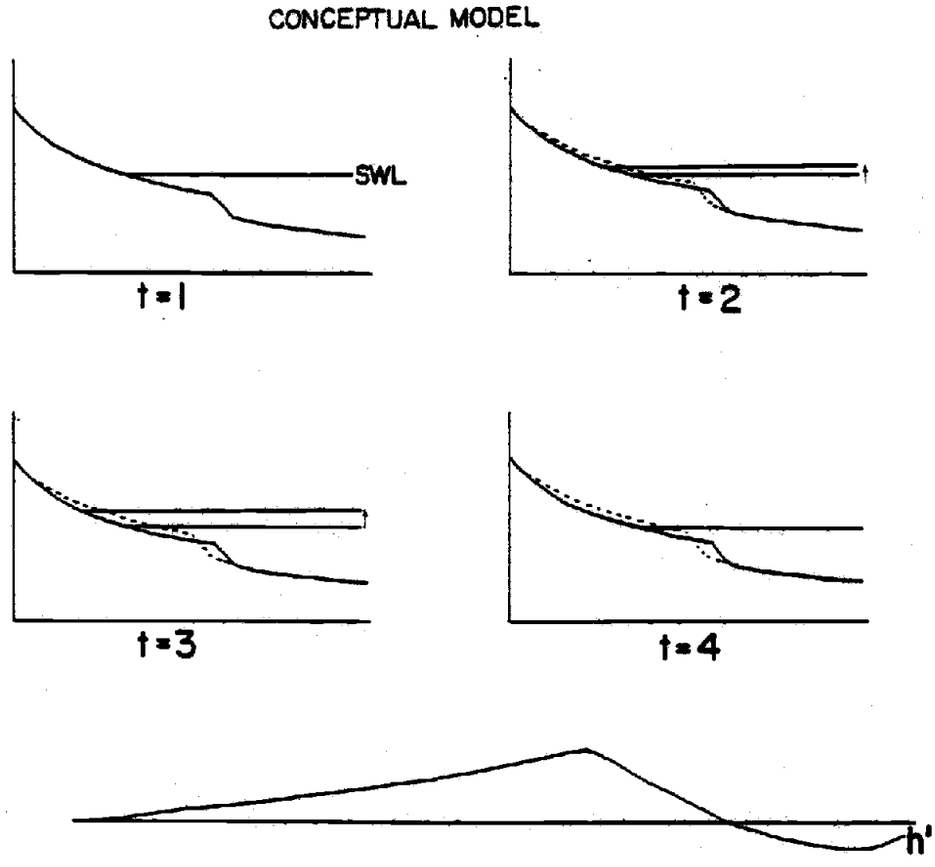

Figure 43. A conceptual model for the formation of the initial perturbation. At t = 1, the foreshore profile is in equilibrium with the runup. A landward shift of the swash-zone results from a long period wave at t = 2. This causes the area of the step to be greatly out of equilibrium. Deposition occurs landward of the original step and erosion occurs on the step itself resulting in a shift toward the profile indicated by the dotted line. This process continues in time 3. At t = 4, the long period wave has receeded to the still water level. This leaves the perturbation shown at the bottom. The perturbation then begins to migrate up the foreshore slope as shown earlier.

SUMMARY

The objective of the field study was to document the influence of infragravity and longer waves on the foreshore profile. The data collected show oscillations of sediment level with maximum heights of nearly 6 cm. The oscillations decrease in amplitude as they migrate in a landward direction.

Evidence suggests that the forcing of these oscillations is the result of long period waves. Low-pass filtered time series of the runup obtained from time-lapse photography show wave forms with the proper characteristics, namely that they preceed the sediment level fluctuations in time and the are of the same apparent period. Figure 21 shows these relationships.

A computer simulation model was based on equations of sediment transport and on a model of runup velocities and distance through time. The model results account for the trends seen in the field data. The modeled perturbations progress in a landward direction, decrease in amplitude and in the rate of migration as they progress. The role of changes in the grain size on the foreshore, both in space and in time were examined and found to be capable of producing changes in the rate of migration and in the apparent

frequency of oscillations, respectively.

The conclusions of this study are that perturbations in the equilibrium foreshore profile are formed near the step in response to a shift in the runup velocity field. The perturbation migrates due to deposition on slopes which are less than what would be in equilibrium, with erosion on greater slopes. The maintainence of the form during progression stongly suggests that some sort of forcing exists throughout the migration. A time-dependant model of perturbation migration is consistent with the observed field data. It suggests that the response time of beaches may be very short. This may be of significance in the study of the formation of more complex topography in the surf-zone.

REFERENCES

Bailard, J.A. and D.L. Inman (1981). An energetics bedload model for a plane sloping beach: local transport. Journal of Geophysical Research, 86: 2035-2043.

Birkemeier, W.A., A.E. DeWall, C.S. Gorbics, and H.C. Miller (1981). A Users Guide to CERC's Field Research Facility. Miscellaneous Report No. 81-7 U. S. Army, Corps of Engineers, CERC, Fort Belvoir, Va.

Baba, J. and P.D. Komar (1981). Measurements and analysis of settling velocities of natural quartz sand grains. Journal of Sedimentary Petrology, 51: 631-640.

Bagnold, R.A. (1963). Mechanics of marine sedimentation. In The Sea, ed. M.N. Hill, 3: 507-528. Interscience, New York.

Bagnold, R.A. (1966). An approach to the sediment transport problem from general physics. Professional Paper 422-1. U.S. Geological Survey, Washington, D.C.

Bowen, A.J. (1980). Simple models of nearshore sedimentation; beach profiles and longshore bars. In The Coastline of Canada, ed. S.B. McCann. Geological Survey of Canada.

Bowen, A.J., and D.L. Inman (1971). Edge waves and crescentic bars. Journal of Geophysical Research 86: 8662-8671.

Branner, J.C. (1900). The origin of beach cusps. Journal of Geology 8: 615-627.

Broome, R. and P.D. Komar (1979). Undular hydraulic jumps and the formation of backwash ripples on beaches. Sedimentology 26: 543-559.

Davis, J.C. (1773). Statistics and Data Analysis in Geology. John Wiley and Sons, New York, NY, 550 p.

Dolan, R., B. Hayden, and W. Felder (1979). Shoreline periodicities and edge waves. Journal of Geology 87: 175-185.

Duncan, J.R. (1964). The effects of water table and tide cycle on swash-backwash sediment distribution and beach profile development. Marine Geology 2: 168-187.

Emery, K.O., and J.F. Foster (1948). Water tables in marine beaches. Journal of Marine Research 7: 644-654.

Evans, O.F. (1938). The classification and origin of beach cusps. Journal of Geology 46: 615-627.

Grant, U.S. (1948). Influence of the water table on beach aggradation and degradation. Journal of Marine Research 7:655-660.

Guza, R.T., and D.L. Inman (1975). Edge waves and beach cusps. Journal of Geophysical Research 80: 2297-3012.

Harrison, W. (1969). Empirical equations for foreshore changes over a tidal cycle. Marine Geology 7: 529-551.

Hibberd, S., and D.H. Peregrine (1979). Surf and runup on a beach: a uniform bore. Journal of Fluid Mechanics 95: 323-345.

Holman, R.A., and A.J. Bowen (1983). Bars, bumps, and holes: Models for the generation of complex beach topography. Journal of Geophysical Research 87: C1 457-468.

Holman, R.A., and R.T. Guza (in press). Measuring runup on a natural beach. Journal of Coastal Engineering.

Huntley, D.A., and A.J. Bowen (1978). Beach cusps and edge waves. Proceedings of the 16th Coastal Engineering Conference, ASCE 1378-1393.

Komar, P.D. (1973). Observation of beach cusps at Mono Lake, California. Geological Society of America Bulletin 84: 3593-3600.

Komar, P.D. (1976). Beach Processes and Sedimentation. Prentice-Hall, Inc., Englewood Cliffs, NJ.

Lanyon, J.A., I.G. Eliot, and D.J. Clarke (1982).Observations of shelf waves and bay seiches from tidal and beach groundwater-level records. Marine Geology 49: 23-42.

Miller, R.L. (1968). Experimental determination of runup of undular and fully developed bores. Journal of Geophysical Research 73: 4497-4510.

Sallenger, A.H. (1979). Beach cusp formation. Marine Geology 29: 23-37.

Sallenger, A.H., and B.M. Richmond (in press). High-frequency sediment level oscillations in the swash zone. Sedimentary Geology.

Shen, M.C. and R.E. Meyer (1963). Climb of a bore on a beach 3: Run-up. Journal of Fluid Mechanics 16: 113-125.

Sonu, C. (1973). Three dimensional beach changes. Journal of Geology 81: 42-64.

Strahler, A.N. (1966). Tidal cycle of changes on an equilibrium beach. Journal of Geology 74: 247-268.

Tanner, W.F. (1965). High-index ripple marks in the swash zone. Journal of Sedimentary Petrology 35: 968.

Tanner, W.F. (1977) Froude regimes in the swash zone. In Coastal Sedimentology ed. W.F. Tanner, Geology Department, Florida State University, Tallahassee, FL.

Waddell, E. (1973). Dynamics of swash and its implications to beach response. Lousiana State University Coastal Studies Institute Technical Report 139. 49 p.

Waddell, E. (1976). Swash-groundwater-beach profile interactions. In Beach and Nearshore Sedimentation eds. R.L. Davis and R.L. Ethington. Society of Economic Paleontologists and Mineralogists Special Publication 24: 115-125.

Wright, L.D., J. Chappell, B.G. Thom, M.P. Bradshaw, and P. Cowell (1979). Morphodynamics of reflective and dissipative beach and inshore systems: Southeastern Australia. Marine Geology 32: 105-140.